An Assessment of Wintering Waterfowl Use of Wetland Reserve Program Restored Wetlands in California Using NEXRAD Weather Radar: Final Report

Jeffrey J. Buler[1], Wylie C. Barrow, Jr.[2], and Lori Randall[2]

November 2010

[1] Department of Entomology and Wildlife Ecology, University of Delaware, 531 S. College Ave, Newark, DE 19716; jbuler@udel.edu

[2] U.S. Geological Survey, National Wetlands Research Center, 700 Cajundome Blvd, Lafayette, LA 70506; wylie_barrow@usgs.gov, lori_randall@usgs.gov

The work on which this report is based was performed in accordance with a cooperative agreement between the U.S. Geological Survey and the University of Delaware.

Table of Contents

List of Figures

List of Tables

EXECUTIVE SUMMARY

The current network of weather surveillance radars (NEXRAD) within the United States readily detects flying birds and has proven to be a useful remote-sensing tool for ornithological study. Previous research developed an approach to quantifying migrating land bird densities by adjusting radar reflectivity measures of birds shortly after the onset of nocturnal migratory flight for biases caused by the vertical distribution of birds in the airspace and radar beam geometry. Our first objective was to apply this approach to evaluate how well the diurnal distributions of wintering waterfowl could be quantified using NEXRAD measures of waterfowl at the onset of their regular evening flights. We also developed a new procedure that locally interpolates radar measures to the same relative time point with respect to sun elevation because flights are closely synchronized with local sunset. We examined the progression of evening flight to select a target sampling time that optimized the spatial accuracy and precision of radar measures and the maximum detection range of birds. We then assessed correlations between bias-adjusted radar reflectivity measures from two radars (KDAX and KBBX) and the diurnal density of waterfowl at the ground based on the locations of radio-marked mallards and northern pintails collected within the Central Valley of California (CVC) during winters 1998-1999 and 1999-2000. Mean time of evening flight initiation occurred 23 min after sunset with the strongest correlations between reflectivity and observed bird density on the ground occurring almost immediately after flight initiation. The effective spatial precision of radar data became coarser over time as birds dispersed from their ground sources. The mean maximum detection range of birds was stable during the first 20 min of flight at 83 km. Therefore, we selected the sun elevation angle of -5º (28 min after sunset) as our target sampling time for quantifying waterfowl distributions. At this sampling time, radar reflectivity was moderately and positively related to the observed diurnal abundance of radio-marked waterfowl locations at the ground.

After establishing that radar measures could serve as an index to waterfowl density, our second objective was to quantify the change in wintering waterfowl density before and after restoration at Wetland Reserve Program (WRP) sites within the CVC to evaluate factors affecting the response of waterfowl to wetland restoration efforts. We analyzed Level II radar data from the NCDC archive

collected during the period of peak wintering waterfowl population numbers for KDAX (winters 1995 through 2007, $n = 13$) and KBBX (winter 1996 – 1998, and 2004 – 2007, $n = 7$). Daytime use by waterfowl at nearly all (84%) sampled WRP sites increased immediately after wetland restoration and for an average of 3 years post-restoration by 469 ± 94% to densities 3.79 ± 1.67 times that of existing wetlands. Thus, WRP sites provide habitat for wintering waterfowl within the CVC. However, the magnitude of the response to restoration by waterfowl varied considerably among sites and was closely related to the amount of surrounding wetland habitat in the local landscape, site wetness (hydrology), the proximity of the site to flooded rice fields, and, most importantly, to pre-enrollment bird density. Sites with high baseline bird density before enrollment had high bird density after restoration. However, bird density after restoration also increased with less surrounding wetland area within a 1.5 km radius, greater increase in site wetness after restoration, and closer proximity to flooded rice fields. Thus, maximizing waterfowl use of WRP sites can be achieved by locating sites close to flooded rice fields within local landscapes with high general waterfowl abundance and relatively little existing wetland area and by intensively managing moist-soil at the site. We developed a map as a decision support tool for prioritizing future WRP enrollments that predicts the post-restoration magnitude of waterfowl use based on the site and local landscape variables associated with relative waterfowl use. Changes in waterfowl distributions during the past 15 years and the increasing importance of flooded rice for waterfowl should be considered for future WRP enrollment strategies.

INTRODUCTION

The Wetlands Reserve Program (WRP) of the U.S. Department of Agriculture (USDA) is a conservation program that aims to create quality habitat for wildlife by offering landowners the opportunity to protect and restore wetlands. The USDA is currently engaged in an effort to quantify the environmental benefits of its conservation program practices through the Conservation Effects Assessment Project (CEAP; Mausbach and Dedrick 2004). Although a few published and unpublished studies indicate greater positive wildlife response to restored WRP wetlands than expected, our understanding of the effect of the more than 1.6 million acres of land enrolled in the WRP nationwide on local and regional population dynamics and habitat use of wildlife is poor (Rewa 2005). Moreover, because interest by landowners has outpaced available funding for enrolling lands, a better understanding of wildlife-habitat relations will aid the limited selection of new enrollments and restoration planning activities within a landscape context to maximize the benefits to wildlife.

Most WRP wetlands are concentrated within a few geographic regions, including the Central Valley of California (CVC), one of the most important waterfowl wintering areas in North America. Given that waterfowl populations have been well-studied and monitored within the CVC (Fleskes et al. 2005b) and waterfowl will use restored wetlands (Stevens et al. 2003, Rewa 2005), there is great potential and importance in assessing the benefits of restored wetlands to waterfowl in the CVC.

Wintering waterfowl, especially field-feeding species such as mallards (*Anas platyrhynchos*) and northern pintails (*A. acuta*), regularly engage in flights between habitats used mainly for resting and those used for feeding (Paulus 1988). Dynamics of these feeding flights have been studied throughout North America, including the agricultural/wetland habitat systems of the West Gulf Coastal Plain and the CVC. Although there is interspecific, geographic, and intraseasonal variability in the exact timing of these feeding flights (e.g., Tamisier 1976, Miller 1985), these movements tend to occur at dawn and dusk and are closely synchronized to sun elevation (Raveling et al. 1972, Baldassarre and Bolen 1984, Ely 1992, Cox and Afton 1996). For example, Baldassarre and Bolen (1984) observed that the evening departures of most individuals of several field-feeding duck species wintering in Texas occurred within a 10 to 15

minute period initiated, on average, 25 ± 2.0 min after sunset. Because of the abrupt *en masse* exodus of waterfowl during evening flights, the opportunity exists to quantify their distributions (i.e., location and relative density) using a single nearly-instantaneous observation collected by weather surveillance radars.

The current network of weather surveillance radars known as WSR-88D (Weather Surveillance Radar 1988 Doppler) or NEXRAD (NEXt Generation RADar) within the United States readily detects biological targets aloft including birds, bats, and insects, and has proven to be a useful remote-sensing tool for ornithological study (Gauthreaux and Belser 1998, Russell et al. 1998, Diehl et al. 2003, Gauthreaux et al. 2003). In particular, these radars have been used to observe the distributions of birds during migratory stopover over large spatial domains by measuring the amount of returned electromagnetic radiation reflected from birds in the radar beam shortly after they leave stopover areas at the onset of nocturnal migratory flight (e.g., Gauthreaux and Belser 2003, Diehl and Larkin 2005, Bonter et al. 2009, Buler and Diehl 2009). Because these migratory flights are closely synchronized to the elevation of the sun (Gauthreaux 1971, Hebrard 1971, Åkesson et al. 1996), bird distributions for a given night are typically sampled using a single nearly-instantaneous radar scan collected during the abrupt *en masse* exodus of birds. Using this approach, Buler and Diehl (2009) demonstrated that radar reflectivity measures are strongly correlated with ground observations of migrant land bird densities and provide relative bird density measures that can be quantitatively compared across the radar area after being adjusted for biases caused by the vertical distribution of birds in the airspace and radar beam geometry.

Developing a robust approach for using weather surveillance radars to quantify waterfowl distributions requires an explicit examination of how evening bird flights develop and are observed by radars to identify an optimal sampling moment during flight initiation. This optimal sampling time should balance potential conflicts between the accuracy and spatial precision of radar data measures, and the effective sampling area of the radar. These three factors can be assessed, respectively, by measuring the correlation between reflectivity and observed bird density on the ground, the geographic specificity of reflectivity measures (i.e., the spatial scale at which the radar effectively resolves bird distributions), and the maximum detection distance of birds. For example, the maximum distance that the radar detects birds

is a function of the height of birds in the airspace and the height of the bottom of the radar beam, which increases with distance from the radar. Because the height of birds in the airspace likely increases as evening feeding flight develops, the maximum detection range should increase with time, allowing one to quantify bird distributions over a greater area. However, the magnitude of the displacement of birds from their ground source also increases with time. This should reduce both the correlation of reflectivity with bird ground density and the geographic specificity of the radar data.

Assessing the accuracy and precision of radar-based estimates of relative bird density requires data of known bird densities on the ground over a large spatial extent. Previously, Fleskes et al. (2005b) tracked day and night locations of individual radio-marked northern pintail and mallard within the northern CVC. These two species comprised 52% (36% and 16%, respectively) of all dabbling ducks observed within the northern CVC during the studied winters based on mid-winter surveys conducted by California Department of Fish and Game and U.S. Fish and Wildlife Service. Thus, distributions of mallards and pintails would likely be representative of the population of waterfowl engaging in evening feeding flights and locations of the radio-marked ducks span the radar areas of two nearby WSR-88D stations. This telemetry dataset provides a unique opportunity for assessing the accuracy and precision of weather radar observations for quantifying waterfowl distributions at two radars among two replicate years.

OBJECTIVES

Our goal was to conduct a quantitative assessment of wintering waterfowl response to wetland restoration within the CVC using weather surveillance radar data through two objectives. The first objective was to develop and validate an improved approach for using weather surveillance radar to quantify wintering waterfowl distributions at the onset of evening feeding flights. To do this, we first examined the progression of evening feeding flights as observed by weather surveillance radar to optimize the sampling time of birds. We then assessed the spatial association between bias-adjusted measures of radar reflectivity and the diurnal density of waterfowl at the ground as determined from a pre-existing dataset of radio-marked bird locations. After establishing that radar measures could serve as

an index to waterfowl density, our second objective was to quantify the change in radar-observed waterfowl density before and after restoration at WRP sites to evaluate the effectiveness of wetland restoration sites (individually and collectively) for their ability to support wintering waterfowl. We also identified local WRP site characteristics and landscape-scale variables that were associated with the greatest increases in relative waterfowl use at sites for consideration when prioritizing the location of future WRP enrollments.

STUDY AREA

The CVC provides critical wintering habitat for many species of waterfowl in the Pacific Flyway. Agricultural and human development have reduced the extent of the estimated 1.6 to 2 million hectares of original wetlands in the CVC by ≥ 90%. However, many wetlands in the northern CVC were converted to rice, corn, or other grain that have high forage value to waterfowl (U.S. Fish and Wildlife Service 1978), resulting in a landscape where waterfowl roost on wetlands and feed in surrounding croplands.

Based on data provided by the Natural Resources Conservation Service (NRCS), between 1992 and 2005, there were 146 individual easements, primarily agricultural fields, enrolled into WRP that comprise ≥ 27,500 hectares within the CVC. Wetland restoration had been completed at 106 sites (72%) as of 2007. Overall, the land area in easements has been restored mostly to emergent wetlands (60%), followed by upland grassland (35%) and riparian forested wetland (5%). The restoration efforts primarily involved physically manipulating micro-topography to restore a more natural hydrological regime, and active winter flooding of easements (J. Groves, personal communication). Restored WRP wetland habitat comprises 8% (12,286 ha) of the total wetland habitat within the CVC based on the 2001 National Land Cover Dataset.

We studied observations from two WSR-88Ds (KDAX; 38.50111°N, 121.67778°W, and KBBX; 39.49611°N, 121.63167°W) located near Sacramento, California that provide radar coverage of the northern half of the CVC (Figure 1). There is a third WSR-88D (KHNX) that provides coverage within the southern CVC that we originally thought would be useful. However, we decided to exclude it from the study because there was insufficient bird activity near the radar to accurately determine vertical bird density profiles for adjusting radar measures and a short effective sampling range due to the high scanning angle of the KHNX radar that precluded many WRP easements from being assessed.

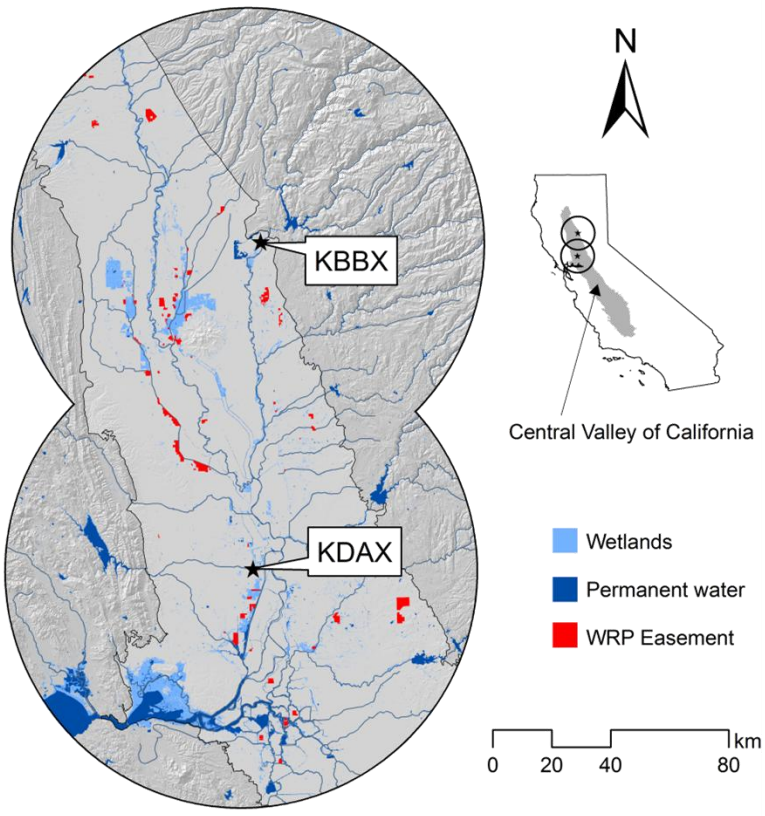

Figure 1. Locations of two WSR-88D stations and their 80 km radius sampling areas within the Central Valley of California. The extent of wetlands and permanent open water during 2000, and Wetland Reserve Program easements as of 2007 also displayed. Black line denotes valley boundary.

Just over half (15,500 ha) of the total area of WRP easements is within the sampling area of KDAX and KBBX. The restored wetland habitat of these WRPs comprises 11% (9,950 ha) of the total wetland habitat within the radar sampling area based on the 2001 National Land Cover Dataset. We selected WRP easements for which we could obtain at least 3 winters of baseline radar data before enrollment and at least one winter of radar data after wetland restoration for analysis. This left us with 43 individual easements that comprised 31 % (4,800 ha) of the total WRP area within the radar sampling area. Many individual WRP easements are directly adjacent to other easements or spatially clustered into restored wetland complexes. Therefore, we grouped selected WRP easements with boundaries located within 4 km of each other into 19 independent sampling units.

OBJECTIVE 1: Quantifying wintering waterfowl distributions using weather radar

METHODS

Weather Surveillance Radar Data: We obtained Level II radar data collected during the period of peak wintering waterfowl population numbers for the winters[1] of 1998 at KDAX and KBBX, and 1999 at KDAX from the data archive hosted by the National Oceanic and Atmospheric Administration's (NOAA) National Climatic Data Center (NCDC; http://www.ncdc.noaa.gov/nexradinv/). WSR-88Ds transmit horizontally-polarized electromagnetic radiation at a wavelength around 10 cm (S band) and a nominal peak power of 750 kW with a half-power beamwidth (3-dB) of 0.95° (Crum and Alberty 1993). The radars measure the strength of the returned radiation in units of Z (reflectivity factor) within sampled volumes of airspace (hereafter referred to as pulse volumes) with dimensions of 1 km in depth by 0.95° in diameter. The Level II data format provides reflectivity measures to the nearest half decibel (0.5 dBZ) for each pulse volume. WSR-88Ds operate in two modes, "clear air" and "precipitation", providing a volume scan comprised of a set of 5 to 14 horizontal 360° sweeps that are each collected at a different elevation angle ranging from 0.5° up to 19.5°. Volume scans are completed every ten or six minutes, respectively, depending on the radar's mode of operation.

We screened radar volume scans to exclude sampling from nights when precipitation was present or there was extreme refraction of the radar beam toward the ground (a.k.a. anomalous propagation) due to non-standard atmospheric conditions. Extreme refraction produces ground returns that contaminate the data and uncertainty in beam height estimation. We also excluded individual pulse volumes where reflectivity measures were regularly compromised due to 1) persistent ground clutter contamination (e.g., radar echoes caused by highway overpasses and wind turbines), 2) radar beam blockage by human infrastructure, or 3) the chronic data filtering that is part of the radar's intrinsic clutter suppression algorithm. We identified these pulse volumes by analyzing reflectivity measures across ~4,000 daytime volume scans collected during the month of June from several years. We analyzed June data because we observed that biological activity in the airspace was at an annual minimum. Specifically, we identified

[1] "Winter 1998" refers to 1 December 1998 through 31 January 1999

compromised pulse volumes for exclusion if reflectivity was measured at a high frequency and with a mean magnitude greater than 1,000 Z, which is indicative of persistent ground clutter, or if reflectivity was infrequently measured regardless of magnitude, which is indicative of beam blockage or chronic clutter suppression. Approximately 20% of quarter-degree pulse volumes were excluded from analysis due to regular contamination.

We processed radar data from suitable sampling days based on the algorithm of Buler and Diehl (2009) that adjusts individual radar measures for several known biases caused by the behavior of birds and the operational characteristics of the radar. First, the algorithm assembles reflectivity measures among volume scans into quarter-degree-wide pulse volumes of fixed azimuth. All further mention of "pulse volumes" refers to these fixed quarter-degree pulse volumes. The algorithm then adjusts reflectivity measures for the differential vertical sampling of birds in the airspace with range from the radar by accounting for the vertical distribution of birds in the airspace and radar beam geometry assuming standard atmospheric conditions. The algorithm characterizes the vertical distribution of birds by determining the mean apparent vertical profile of reflectivity (VPR) based on the method of Andrieu and Creutin (1995). The algorithm also estimates the proportion of birds in the airspace that are sampled within each pulse volume. Only data from pulse volumes that sample >5% of the birds in the airspace were included for analyses. The algorithm incorporates partial beam blockage due to topography when computing adjustment factors for individual pulse volumes. We determined the mean ground height for every pulse volume to the nearest 10 m using elevation data from the National Elevation Dataset assembled by the U.S. Geological Survey. Data from pulse volumes with more than 30% of the radar beam blocked were excluded from analyses.

There remains in this bias-adjustment approach a potential for sampling error among radars and among days at the same radar due to the relatively-coarse sampling rate of WSR-88D (e.g., one radar scan every 6 or 10 min) and for sampling bias within an individual radar scan along an east-west gradient as birds initiate flight over a relatively short time period following local sunset (Diehl and Larkin 2005, Buler and Diehl 2009). For example, across a 160 km diameter area around a radar site at a temperate

latitude (e.g., 38°), local sunset occurs at the eastern extent about 8 minutes before the western extent. Thus, many birds at the eastern extent could be aloft before any birds at the western extent have initiated flight. Additionally, WSR-88D data collection is not synchronized to the onset of bird movements, so there could be up to a 5 minute difference in sampling times relative to a given sun elevation among individual days. Consequently, Buler and Diehl (2009) recommend that future approaches to quantifying bird distributions should reduce sun-elevation-induced sampling error and bias by locally interpolating reflectivity measures to the same relative time point with respect to sun elevation.

Therefore, we interpolated reflectivity measures of each pulse volume within the 5 lowest elevation angle sweeps to a sun elevation angle of 5.0° below horizon for each sampling day. We interpolated data using inverse distance weighting of reflectivity measures based on timing differences between the radar volume scan collected immediately before and the scan collected immediately after the target sun elevation time point. We decided on the target sun elevation of -5.0° after analyzing several characteristics of the timing and progression of feeding flights from a series of interpolated radar measures with sun elevation ranging from 0° (i.e., sunset) to 10° below horizon by half-degree time steps (see Results).

We made the following additional modifications to the algorithm of Buler and Diehl (2009) to further improve the accuracy of reflectivity measure adjustments. When computing beam characteristics, we accounted for the Gaussian distribution of the power in the beam rather than assume uniform power in the beam. Additionally, because a significant part (25%) of radar sensitivity is outside the main 3-dB beam, we modeled beam characteristics using a 6-dB wide beam, which includes 94% of the radar sensitivity. When determining VPRs, we incorporated the variability in mean ground height across ranges into beam height calculations and filtered out data from partially blocked beams. We also identified the effective maximum height of birds in the airspace as the maximum beam height of the 0.5° elevation angle beam at the shortest range from the radar where the mean reflectivity of the 1.5° beam is effectively zero relative to that of the 0.5° beam (i.e., mean reflectivity of 1.5° beam divided by mean reflectivity of 0.5° beam was less than 0.005). Reflectivity values at heights above this effective maximum bird height

were set to zero for determining VPRs. Finally, because reflectivity measures were log-normally distributed, we used geometric means rather than arithmetic means where appropriate.

The culmination of our methodology development was the creation of the software package BIRDS (Bias Improvement of Radar Data System). Originally, we converted raw radar data into dBase data format using NOAA's Weather and Climate Toolkit and wrote programming code to perform the bias adjustment processing of the converted radar data within SAS® 9.1 for Windows (see Buler and Diehl 2009). We later developed BIRDS as a system of Java scripts, Python scripts, and Fortran 95 code to automate data handling and conversion, vastly improve processing time, and allow for the analysis of radar data without reliance on commercial software. BIRDS converts raw radar data to ASCII data format, performs the interpolation (temporally and spatially), computes VPR, and adjusts for reflectivity measure biases.

Radio Telemetry Data: We used 8,076 daytime (based on local sunset/sunrise) locations of waterfowl collected within 100 km of either radar site during December and January 1998-2000 (see Fleskes et al. 2005b for details). Waterfowl were tracked daily from trucks or fixed-wing aircraft throughout the study period. Daytime locations were recorded once a day with an estimated precision of 1.1 ha in area (Warnock and Takekawa 1995). Weekly aerial searches of waterfowl habitat and urban areas throughout the Central Valley were also conducted for missing radio-marked waterfowl. Locations were from a total of 365 individual northern pintail and mallard.

Female after-hatch-year pintails (n = 261) were captured and radio-marked during late August through early October of each study year at three wetland locations; the Colusa Basin in the northern CVC, the Suisun Marsh just to the west of the CVC, and the Grassland Ecological Area and Mendota Wildlife Area in the southern CVC (Figure 2). The Colusa Basin and Suisun

Marsh are within the combined radar coverage area, but individual pintails are highly mobile and, with a mean ± SE dispersal distance from their capture site of 120.9 ± 5.5 km, pintails from all capture sites ranged across the entire study area during the course of a winter.

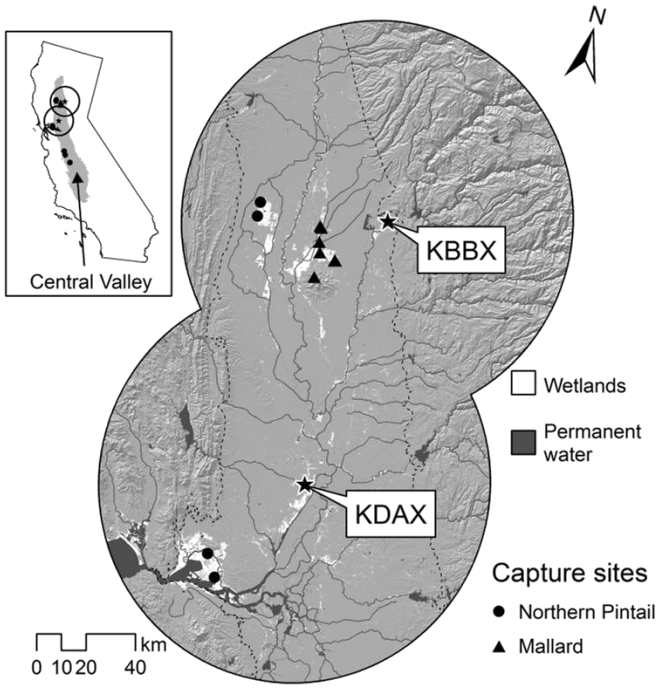

Figure 2. Capture locations of radio-marked northern pintail and mallard within the radar sampling area in the Central Valley of California. Locations and names of WSR-88D stations are shown. Dashed line denotes the valley boundary.

Female after-hatch-year and hatch-year mallards (n = 104) were captured and radio-marked during late August through mid-September of each study year at Graylodge and Upper Butte Basin Wildlife Area in the northern CVC near the KBBX radar. With a mean ± SE dispersal distance from their capture site of 16.0 ± 1.4 km, individual mallards exhibited limited movement compared to pintails and their locations were almost exclusively restricted to within the KBBX radar area. Therefore, we excluded mallard locations for comparisons with radar data from KDAX.

Data Analysis: We evaluated three factors during the progression of flight onset to determine a target sun elevation angle to use when quantifying the relative diurnal density of waterfowl at the ground: 1) the correlation between reflectivity and observed bird density on the ground, 2) the geographic specificity of reflectivity measures, and 3) the maximum detection range of birds. We computed Pearson's correlation coefficient to determine the correlation between the seasonal geometric mean reflectivity (i.e., relative bird density aloft) and the mean kernel density of radio-marked waterfowl locations (i.e., relative waterfowl density on the ground) among individual pulse volumes. We used the quadratic kernel function of Silverman (1986) to create a 30-m-resolution raster grid surface of the density of all radio-marked bird locations during a season, and then averaged kernel density values of grid

cells located within the two-dimensional boundaries of a pulse volume to derive mean kernel density. We computed kernel density of radio-marked birds for a series of bandwidth sizes ranging from 500 m to 10 km by 500 m intervals. To reduce potential problems with spatial autocorrelation of data, we drew random samples of 30 pulse volumes that were separated by ≥ 10 km to generate 2,000 bootstrap samples for the correlation analysis. We then averaged correlation coefficients across the collection of bootstrap samples by radar, bandwidth, and season. We log-transformed data to meet the assumption of a bivariate normal distribution for statistical analysis.

As a relative estimate of the geographic specificity of radar data, we used the bandwidth size of the kernel density of radio-marked bird locations which produced the greatest correlation coefficient with reflectivity. Because the geographic specificity is largely influenced by the dispersal of birds from their ground source (Diehl and Larkin 2005), we also estimated the median dispersal distance of birds aloft for each volume scan. We did this by multiplying the median height of birds aloft, based on the VPR from the radar data processing algorithm, by the product of the mean horizontal ground speed (17.5 m/s) and the mean vertical ascent rate (0.5 m/s) of waterfowl species during climbing flight (Hedenström and Alerstam 1992). This calculation assumes birds fly in a straight line at constant vertical and horizontal speeds during the initiation of evening flights, which is consistent with our visual observations. A violation of this assumption (i.e., birds vary in their ascent rate or engage in a meandering flight path) would lead to an overestimate of median dispersal distance.

As another measure of the geographic specificity of the radar data, we determined the extent of spatial autocorrelation of the radar data using semivariogram analysis (Cressie 1993). We fit the empirical semi-variance among a random sample of 5,000 adjusted reflectivity measures as a function of the distance between pulse volume centroids for each interpolated volume scan using the following isotropic exponential function;

$$\gamma\ h\ = c_o + c_e\ \ 1 - e^{-h/a}\ ,$$

where h is the distance between two measures (i.e., the lag distance), c_o is the variance due to sampling error and/or spatial dependence at distances smaller than the sampling interval (i.e., nugget), c_e is the partial population variance, and a is the range below which data are spatially dependent. The assumptions of normality and stationarity of variance were met by log-transforming and detrending reflectivity measures. We detrended reflectivity values by fitting first-order polynomial models within a local moving window of 15 km radius.

We determined the mean maximum range that the radar detected birds among the subset of azimuths where the radar beam was unobstructed by topography. The detection range for each azimuth was the maximum range at which the radar sampled at least 5% of the birds in the airspace for at least 75% of sampled nights within a season.

RESULTS

Overall, we sampled evening waterfowl feeding flights from 30% (55 of 186) of potential days (Appendix A). We excluded the other 70% percent of days from analyses due to precipitation (28%), missing data in the archive (27%), or anomalous propagation of the radar beam (15%).

We analyzed the onset of evening flights for 45 days from the KDAX radar during winter 1998 and 1999. Beginning at sunset, the magnitude of mean reflectivity across days was relatively moderate (7 times greater than the minimum) and exhibited a stable shallow rate of decline over time (8% per min) until reaching its minimum value when sun elevation reached -4° (23 min after sunset) (Figure 3A). From 23 min after sunset until the end of our sampling time window (56 min after sunset), mean reflectivity increased, indicating increasing relative bird density in the airspace. We considered the start of this increase in reflectivity as the mean initiation time for evening feeding flights. Feeding flight initiation times varied among individual nights, ranging from 11 to 34 min after sunset with a standard deviation of 4 min. As evening flight progressed, the relative rate of change in mean reflectivity increased steeply until reaching a maximum of 24% per min at a sun elevation of -7° (40 min after sunset). Then the rate of increase declined until mean reflectivity reached an asymptotic maximum value 16 times greater than that at the initiation of feeding flight. The geometric mean height of birds above ground derived using

estimated vertical reflectivity profiles closely matched the change in reflectivity after the initiation of feeding flight, increasing from 64 ± 4 m to 91 ± 3 m (Figure 3B).

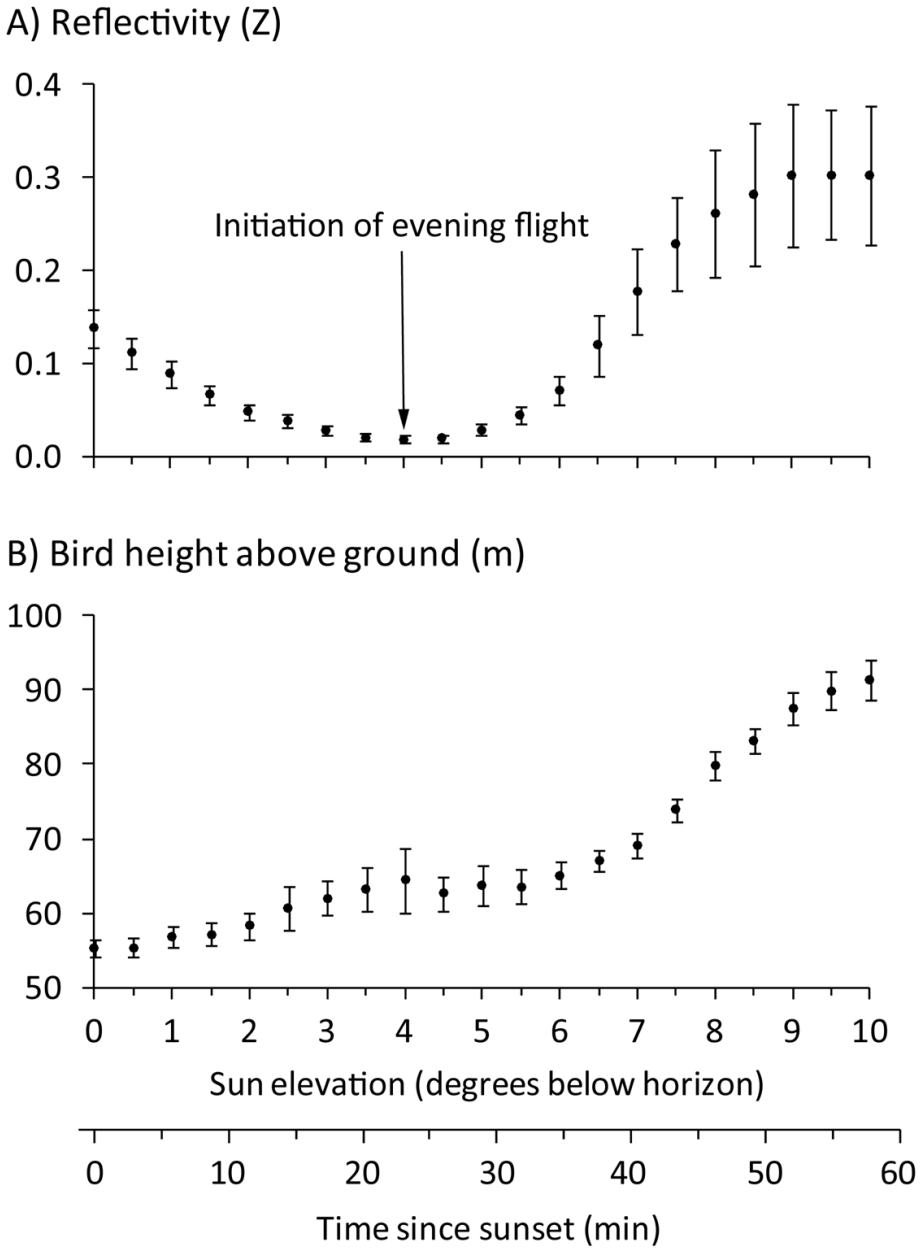

Figure 3. Time series depicting the change in A) mean radar reflectivity (i.e., relative density) and B) mean height of birds aloft during evening flights around the KDAX radar during winters 1998 and 1999 (n = 45).

The sun elevation of -5.0° (i.e., 5 min after flight initiation) was the optimal target sun elevation for quantifying the relative diurnal density of waterfowl at the ground. The seasonal geometric mean reflectivity during both winters was most strongly and positively correlated to the 0.5 km bandwidth (i.e., most specific) seasonal kernel density of radio-marked waterfowl locations on the ground at a sun elevation of -5.0° (Figure 4A). At the initiation of evening flight, the kernel bandwidth distance of ground data that produced the strongest correlation with reflectivity was relatively small among winters, but increased sharply as flight progressed; reaching the maximum evaluated bandwidth of 10 km at a sun elevation of -7.5° (~ 20 min after flight initiation) (Figure 4B). The overall mean maximum detection range of birds was stable and relatively moderate (~83 km) for about 25 min after the initiation of evening flight before increasing thereafter (Figure 4C). During the stable detection range period, median bird height averaged 110 ± 1 m.

At a sun elevation of -5.0°, the strongest correlations between geometric mean reflectivity and the seasonal kernel density of radio-marked waterfowl locations for data from the KDAX radar were 0.61 during winter 1998-99 and 0.54 during winter 1999-00 (Figure 5). The strongest correlation for data from the KBBX radar during winter 1998-99 was 0.62. Spatially, there were close associations between areas of the greatest reflectivities and radio-marked bird densities (Figure 6). We note that the radars also measured a few "hotspots" of high reflectivity where no radio-marked birds occurred, but where unmarked waterfowl do occur (J. Fleskes, pers. observation). The mean kernel bandwidth distance of ground data that produced the strongest correlation between geometric mean reflectivity and the seasonal kernel density of radio-marked waterfowl locations among seasons was 5.0 km. Additionally, for all volume scans pooled across season and radars (n = 55), the estimated median dispersal distance of birds from their ground source was 3.85 ± 0.35 km, and the mean ± SE range (a) of spatial autocorrelation of radar reflectivity was 3.79 ± 0.12 km.

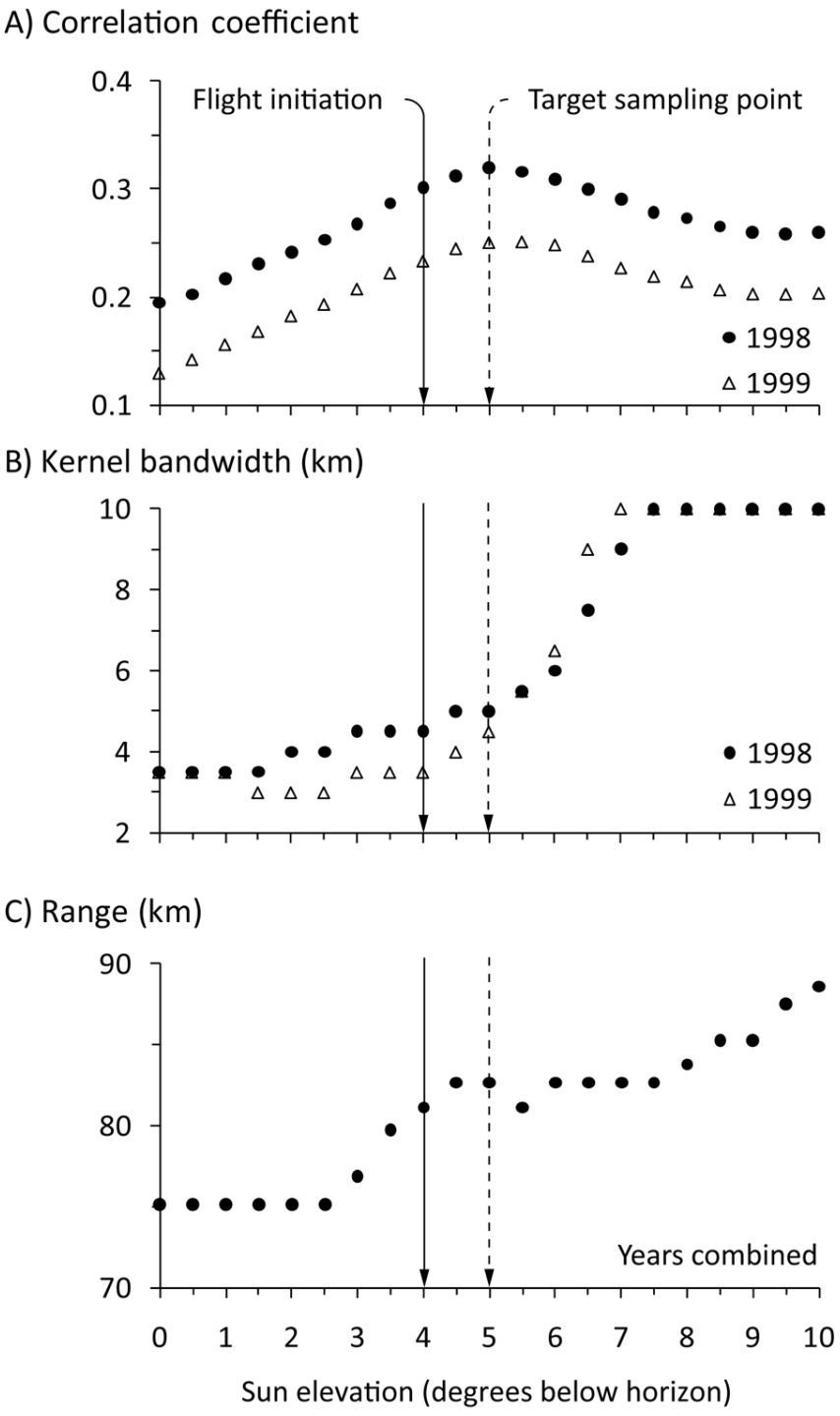

Figure 4. Time series depicting the change in radar data accuracy, specificity, and sampling area as measured, respectively, by A) the mean correlation between geometric mean reflectivity and the mean kernel density of radio-marked waterfowl locations within a 0.5 km bandwidth, B) the bandwidth size of the maximum mean correlation coefficient between geometric mean reflectivity and mean kernel density of radio-marked waterfowl locations, and C) the mean maximum range that the radar detected birds in the airspace during evening flights around the KDAX radar among 2,000 bootstrapped samples of 30 individual pulse volumes during winter 1998 (n = 18) and 1999 (n = 27).

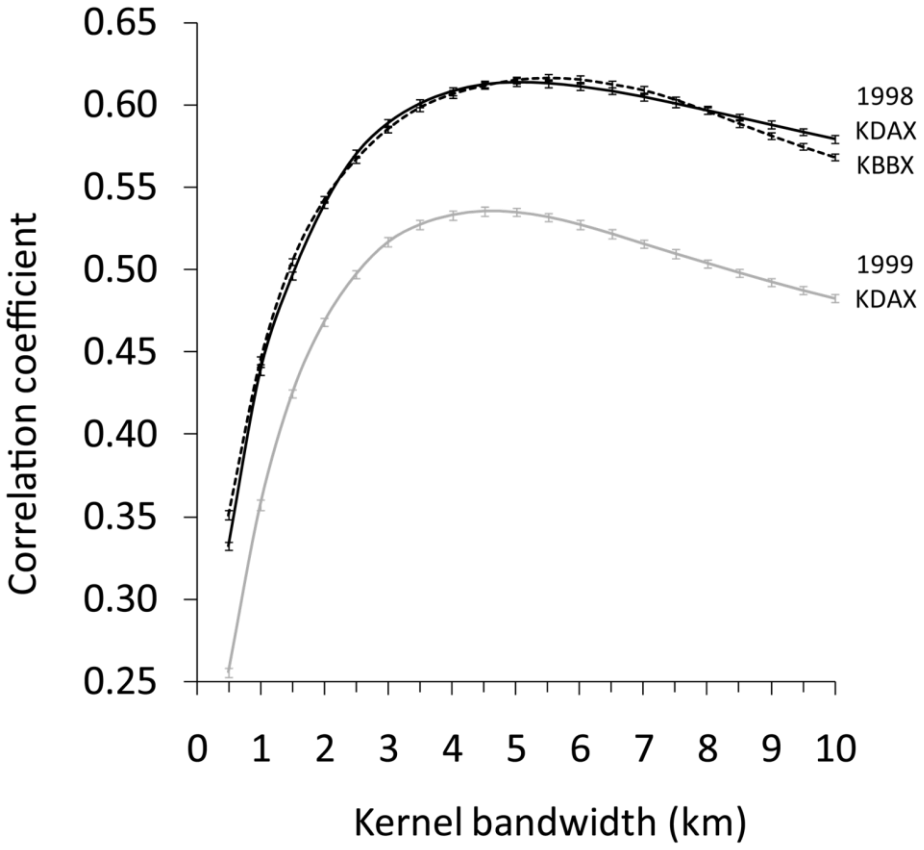

Figure 5. Change in mean correlation between geometric mean reflectivity and kernel density of radio-marked waterfowl locations with respect to the kernel bandwidth distance of ground data by winter and radar. Error bars denote ± 1 standard error of the mean among 2,000 bootstrapped samples.

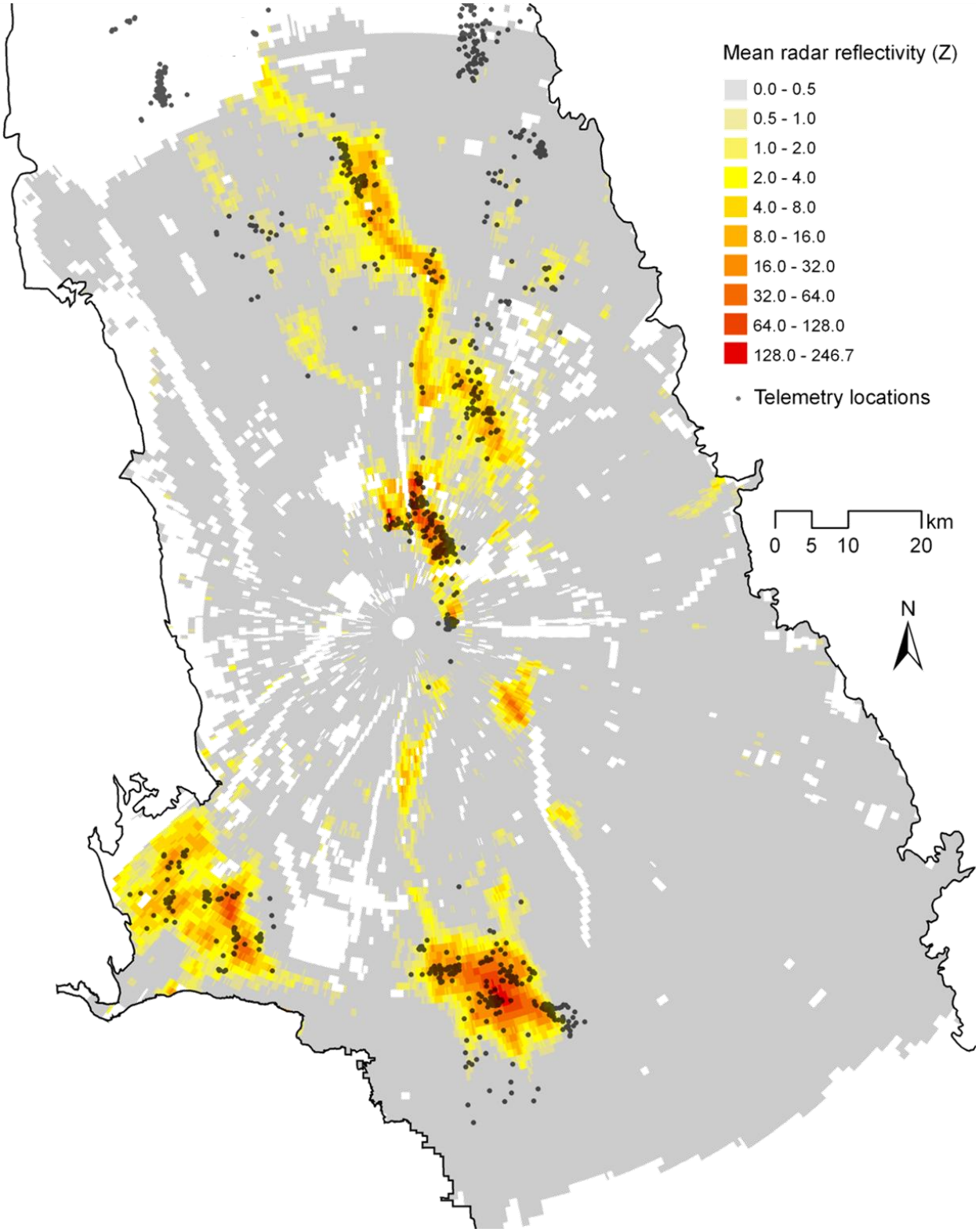

Figure 6. Map of geometric mean reflectivity around the KDAX radar (n = 18 days) and the locations of radio-marked northern pintail (n = 3,102) during winter 1998. White areas denote regions where radar data were excluded from analysis because persistent clutter was present or the radar beam was too high to detect birds aloft.

DISCUSSION

The temporal pattern of radar reflectivity observed by weather surveillance radar was consistent with published observations of crepuscular bird activity and our own visual observations. We attribute the initial post-sunset reduction in relative bird density aloft to the cessation of afternoon flights by geese, waterbirds, and songbirds to roosting sites. During four evenings at various locations throughout the study area in January 2009, we made visual ground observations of greater white-fronted goose (*Anser albifrons*) and white-faced ibis (*Plegadis chihi*) returning after sunset to roosting sites within wetland habitats. Similarly, Ely (1992) observed that greater white-fronted geese within the CVC typically end their afternoon feeding flights within 20 minutes after sunset. Blackbirds, *Agelaius* spp., also engage in afternoon feeding flights that end shortly after sunset within the CVC (Orians 1961). Nearly all the activity of roosting birds in the airspace subsided shortly before we observed waterfowl initiating evening flights. Thus, the cessation of afternoon bird flights did not significantly overlap with the evening waterfowl feeding flight.

The mean initiation time of 23 min after sunset for waterfowl feeding flights based on radar observations fell within the range of initiation times reported by others (Tamisier 1976, Baldassarre and Bolen 1984, Miller 1985, Cox and Afton 1996; Table 1) and corresponded with our ground observations of dabbling ducks initiating flight and leaving wetland habitats. Variability in the timing of evening flights among individual days relative to sun elevation has been associated with weather and light conditions. For example, departures can be 10 to 15 min earlier under completely overcast conditions (Baldassarre and Bolen 1984), or delayed a few minutes when bright moonlight is present (Tamisier 1976, Cox and Afton 1996). However, the standard deviation in the timing of evening flights that we observed among individual days was less than half the magnitude of the relatively-coarse sampling rate of the radar. Thus, sampling birds at a static sun elevation across nights would likely produce results similar to accounting for the variability in the timing of evening flights for individual days.

Although we observed non-waterfowl birds aloft during evening flights, their contribution to radar reflectivity measures is likely minimal. Specifically, we observed black-crowned night-herons

(*Nycticorax nycticorax*) initiating flights concurrent with waterfowl evening flights. Siebert (1951) observed that evening departure of night-herons from diurnal roosting sites coincides with the feeding flights of waterfowl. Non-waterfowl bird species including waterbirds aloft have been observed during winter evening waterfowl feeding flights in Louisiana (W. Barrow, USGS, personal communication). However, waterfowl comprised at least 97% of the birds within the radar beam.

Table 1. Mean evening feeding flight initiation time for wintering dabbling duck species at various locations.

Mean ± SE of flight initiation time (min after sunset)	Species	Location	Study
22 ± 1	northern pintail	Louisiana	Cox and Afton 1996
~25	northern pintail, American green-winged teal	Louisiana	Tamisier 1976
25 ± 2	Primarily northern pintail, mallard, American green-winged teal, American wigeon	Texas	Baldassarre and Bolen 1994
~30	northern pintail	California	Miller 1985

We selected the sun elevation of -5º (28 min after sunset) as our target sampling time for quantifying the relative diurnal density of waterfowl at the ground. We based this primarily on the magnitude of the correlation between reflectivity and observed bird density on the ground and the geographic specificity of the radar data. As expected, the strongest correlations occurred almost immediately after the initiation of evening flight and became weaker over time. Additionally, the geographic specificity of the radar data rapidly became coarser over time as birds continuously streamed from their ground sources and dispersed in variable directions. Because of this dispersal, the associations of birds with their ground sources quickly became blurred and reflectivity measures became homogenized. We doubt that an effective correction for the complicated nature of how waterfowl disperse from their ground source is possible. In contrast, migrating land birds leave their stopover ground sources in a uniform direction, so some adjustment for spatial displacement is possible (Buler and Diehl 2009). Regardless, it seems optimal to sample birds immediately after the initiation of evening feeding flights to achieve the best spatial accuracy and precision when quantifying their approximate ground location.

While we also considered the maximum detection range of birds in selecting the target sampling time, it had little ultimate influence on our selection of a sampling time. This is because the maximum detection range of birds was unexpectedly stable during the critical first 25 min after the initiation of flight, before increasing thereafter as evening feeding flight progressed. During this time birds were likely engaged in a mixture of climbing, descending, and cruising flight due to individual variability in their flight timing and relatively-short travel distances to feeding sites, which resulted in relatively stable bird height distributions in the airspace. Baldassarre and Bolen (1984) observed that the evening departures of most individuals occurred within a 10 to 15 minute period. Additionally, evening feeding flight distances for northern pintail and mallards within the northern CVC average (± SE) 7.00 ± 0.11 km and 3.60 ± 0.06 km, respectively (Fleskes et al. 2005b). Combining these observations with the average flight speed of northern pintails during feeding flights (10.5 m/s) derived from Cox and Afton (1996), we estimate the total mean duration of feeding flight activity of pintails and mallards to be 21 to 26 min and 16 to 21 min, respectively. This corresponds closely to the duration of the period of stable bird height distributions.

The radars observed birds in the airspace for longer than the estimated duration of short-distance feeding flights by dabbling ducks. We believe the radar observed two types of evening flight that were initiated concurrently; short-distance feeding flights and long-distance dispersal flights of waterfowl. While screening radar data, we noticed the radars regularly detected distinct groups of birds moving long distances (e.g., 10's of kilometers) for up to two hours after the initiation of evening flights and well after the subsidence of short-distance feeding flights. This activity also corresponded to the increase in mean bird height in the airspace after feeding flights subsided. Northern pintails (Fleskes et al. 2002, Miller et al. 2005) and white-fronted geese (Fleskes et al. 2005b) are known to move widely among basins throughout the CVC during winter. The long-distance flight observed by the radar may be those of waterfowl dispersing to other wintering areas within the CVC.

At our target sampling time, we found that radar reflectivity measured at the onset of nocturnal waterfowl flight was positively spatially related to the observed diurnal abundance of radio-marked waterfowl locations at the ground. Admittedly, the radio-telemetry dataset was not designed or collected

for the purpose of ground-truthing radar observations. Consequently, the moderate correlations we found were likely constrained by the extent that our opportunistic dataset of radio-marked pintail and mallard distributions represented the distributions of all birds engaging in evening flights. We encourage the collection of more-robust ground-truthing data in the future. This would allow for assessing the accuracy and precision of weather radar observations for quantifying waterfowl distributions with greater certainty. Regardless, these results complement close temporal correlations between radar reflectivity and observed waterfowl density in the airspace within and across days (O'Neal et al. 2010, W. Barrow, USGS, personal communication). Thus, radar reflectivity can be used as a relative index of wintering waterfowl density for quantifying waterfowl distributions across space and time.

Two important advantages of using weather surveillance radars to sample waterfowl distributions compared to traditional survey approaches are that radars provide comprehensive coverage over large areas, including remote areas that are difficult to access, at minimal cost (Ruth et al. 2008), and their measures are not subject to biases due to observer variability and bird visibility (Pollock and Kendall 1987, Johnson et al. 1989, Thompson 2002). We found the radars could effectively detect birds out to 83 km in regions with little topographic relief. This is similar to the detection range of 80 km when using WSR-88D to quantify land bird distributions during migratory stopover (Buler and Diehl 2009). However, effective radar coverage for some areas within this maximum detection range may not be available due to partial or complete blockage of the radar beam from topographic relief or human infrastructure near radar sites. Radar measures are subject to their own suite of known biases (see Diehl and Larkin 2005) primarily due to beam geometry and the distribution of birds in the airspace. These measurement biases can be accounted for in large part using the approach originally proposed by Buler and Diehl (2009), and improved upon in this study.

An important limitation of weather surveillance radar is the effective spatial resolution of the data, which is relatively coarse and not well suited for examining fine-scale or site-specific patterns (Ruth et al. 2008). The extent of dispersion of birds from their ground sources determines the effective spatial scale at which bird distributions can be quantified (Diehl and Larkin 2005). Consistent with this view, our

estimate of median dispersal of birds from their ground source at the target sampling time was nearly identical to the scale of spatial autocorrelation of the radar data and on the same order of magnitude as the scale at which the kernel density of radio-marked waterfowl locations was most strongly correlated to the radar data. Despite spatial autocorrelation in the radar data out to about 4km, finer-scale associations of birds with their ground sources can be resolved, particularly where discrete patches of suitable habitat exist in an unsuitable matrix and when summarizing data across sampling nights (Figure 7). Associations of birds from habitat patches or sites that are smaller than the dimensions of the sampling radar pulse volume are not possible because their contribution to total reflectivity in the measured airspace is diluted and contaminated from birds emanating from other areas within and outside the pulse volume.

Our results show that WSR-88D data are useful for detecting change in habitat use by waterfowl related to disturbance (e.g., hunting) and land use change, and could be used to measure waterfowl response to habitat management programs that are usually obtained via surveys or radiotracking. The data archive going back to the mid 1990's allows for research that requires multiple years of data and/or retrospective baseline data. Currently, annual estimates of regional wintering waterfowl abundance and distribution are obtained via aerial surveys. However, limited availability of trained observers and cost and danger of conducting aerial surveys may limit their future use. Analysis of radar data like we report here, perhaps supplemented with other data that better determines species composition, may be a feasible replacement.

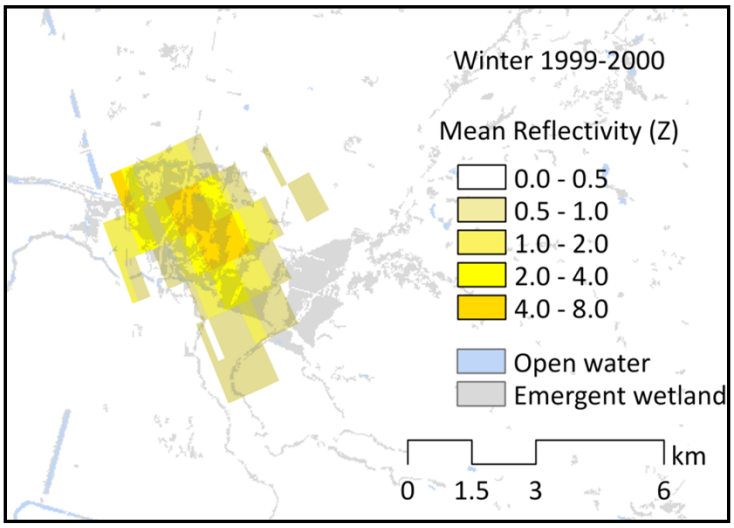

Figure 7. Map of radar reflectivity associated with a wetland habitat patch complex during winter 1999.

We are currently developing a user-friendly graphical interface for the BIRDS software and plan to make it freely available for distribution in the near future for operation on desktop PCs. Users will be able to input the uncompressed Level II radar data files available from the NOAA NCDC archive and

output bias-adjusted radar data in file formats easily imported into popular statistical or GIS software. This will enable non-technical users interested in processing WSR-88D data for quantifying bird distributions to pursue their own management related research questions and analyses.

OBJECTIVE 2: Assessment of wintering waterfowl response to wetland restoration at Wetland Reserve Program sites

METHODS

Weather Surveillance Radar Data: We obtained all available Level II radar data from the NCDC archive collected during the period of peak wintering waterfowl population numbers for KDAX (winters 1995 through 2007, n = 13) and KBBX (winter 1996 – 1998, and 2004 – 2007, n = 7). Following the same methods from Objective 1, we 1) screened radar volume scans to exclude sampling from nights when precipitation was present or there was anomalous propagation of the radar beam, 2) interpolated reflectivity measures to a sun elevation angle of 5.0° below horizon, and 3) applied modifications to the algorithm of Buler and Diehl (2009) to further improve the accuracy of reflectivity measure adjustments. As a measure of relative bird density for each winter, we calculated the geometric mean reflectivity (x) across sampling days (i) at each pulse volume since reflectivity measures (x) were log-normally distributed using the following formula;

$$x = \exp\ \frac{1}{n}\ \ \sum_{i=1}^{n} \ln x_i\ .$$

To control for annual fluctuations in overall waterfowl populations and their use of wetlands, we standardized relative bird density measures for a given winter by dividing the mean winter reflectivity for a pulse volume by the overall mean winter reflectivity among all pulse volumes whose 2-dimensional extent over land was comprised primarily of wetland habitat (≥ 85%) based on land cover data from 1999 (described later). This produced standardized bird density measures expressed as the ratio of reflectivity relative to that of wetland habitats where a value of 1 indicates bird density identical to that at existing wetlands.

Land Cover and Wetness Index Data: We used the 1999 land cover dataset produced by Fleskes et al. (2005a) to determine the distribution of habitats within the CVC. This dataset was derived from 30 m resolution Thematic Mapper (TM) data and classified land cover into the following types: rice, non-rice agriculture, permanently- and seasonally-flooded wetlands, open water, grass, barren, and other. We combined the two wetland types into a single "wetland" category. We chose this land cover dataset over others that are available (e.g., National Land Cover Dataset, California GAP Analysis) because rice is classified separately from other types of agriculture and the year of data collection is close to the middle of the time period of our study. One caveat to our analyses is that we treat land cover as static for the entire time period.

We used satellite sensing of surface water, which is possible in areas where vegetation and cloud cover do not obscure water (Smith 1997, Alsdorf et al. 2007), to quantify the annual fluctuations in the extent of surface water and soil moisture. We screened all available winter Landsat TM 5 and 7 satellite data from the USGS EROS Data Center. We focused on obtaining at least one cloud-free image per winter between December 1 and January 31 that coincided with peak abundance of wintering waterfowl. Cloud-free TM images were not available for winters 1995 and 1997. We calculated a mean wetness index among images for each winter using the Tasseled Cap transformation of Huang et al. (2002) for TM 7 data and Crist (1985) for TM 5 data (Figure 8A). This index has been shown to be sensitive to soil and plant moisture and increases positively with moisture, with open water on the surface having positive index values (Crist and Cicone 1984). We calculated the mean wetness index within WRP easement boundaries during each available winter. We also quantified the extent of flooded rice during each winter by integrating the map of classified surface water based on wetness index (Figure 8B) with the land cover map (Figure 8C).

The vast majority of WRP lands are under some degree of moist soil management categorized as either active or passive, depending largely on the frequency of soil disturbances and intensity of water level manipulation. Additionally, rice fields within the valley are subject to active and passive flooding during winter. For actively flooded WRP and rice fields, water is usually put on the fields during October

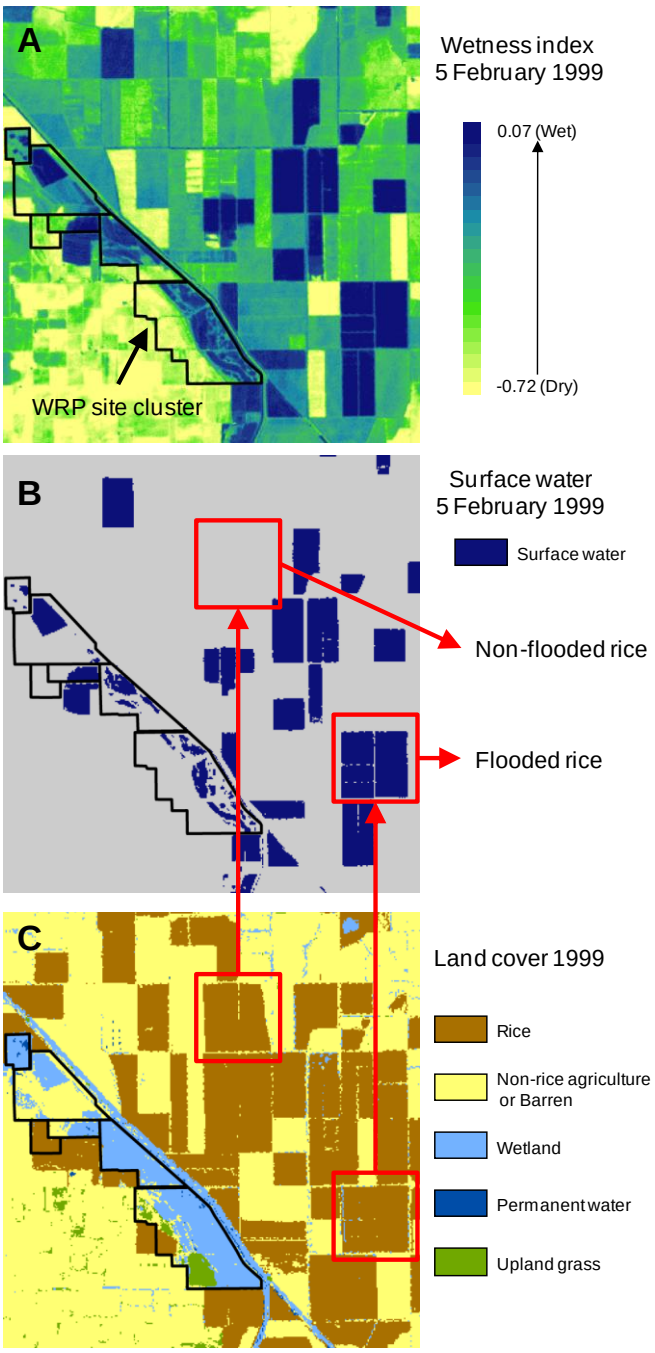

Figure 8. Example data layers of A) wetness index, B) surface water, and C) land cover. Red squares and arrows illustrate how surface water and land cover data were integrated to determine extent of flooded rice.

for rice decomposition and/or duck hunting leases. This water is normally retained on fields until early February when hunting season ends. The extent of flooding fluctuates annually depending on water supplies, but is fairly stable within winters. Thus, active flooding at WRP sites can be determined with a single winter TM image. Passive flooding/puddling of fields varies with valley rains and snow melt both among and within winters (J. Fleskes, personal communication) and is less accurately quantified using a single winter TM image.

Data Analysis: We grouped data from individual years into three classes based on enrollment and restoration status. Data from winters prior to enrollment of a WRP easement when active farming was being conducted were classified as "pre-enrollment" years. Winters after enrollment but prior to completion of wetland restoration when there was no active farming nor habitat management were classified as "enrollment" years. Winters following the completion of restoration efforts were classified as "post-restoration" years. We determined the mean standardized bird density across years by restoration class for each WRP site cluster as follows: We first used an area-weighted average of standardized bird density among pulse volumes within the easement boundary. We then averaged these

means among easements within each cluster weighted by easement area. Mean restoration age of each WRP site cluster was determined by calculating the area-weighted mean restoration age among individual easements within the cluster. We also determined the change in bird density after restoration by subtracting the mean standardized bird density during pre-enrollment years from the mean standardized bird density during post-restoration years.

We applied multi-model inference within an information-theoretic approach to estimate the relative importance and effect size of predictor variables in explaining variation of the mean standardized bird density during pre-enrollment and post-restoration years, and the relative change in mean standardized bird density after restoration using simple linear models (Burnham and Anderson 2002). Predictor variables included local site, landscape composition, and landscape placement characteristics. Local site characteristics analyzed for pre-enrollment data included mean wetness index and site area. Local site characteristics analyzed for post-restoration data included mean standardized bird density during pre-enrollment years, change in mean wetness index before and after restoration (i.e., post-restoration mean wetness index minus pre-enrollment mean wetness index), restored wetland area, and the mean age of restoration. Landscape composition variables included the amount of wetland, flooded rice, and open water surrounding sites. For each landscape composition variable, we determined the radius around sampling sites at which each predictor variable was most strongly correlated to the response variable among the set of radii ranging from 0.5 km to 4 km at 0.5 km increments (sensu Holland et al. 2004). Landscape placement variables included the proximities of the site to the nearest flooded rice field and the nearest wetland.

Because a balance in the number of models that contain each variable is desirable when determining relative variable importance, we tested all possible subsets of models excluding interaction terms. We used Akaike's Information Criterion adjusted for small sample sizes to rank models based on their ability to explain the data, and used Akaike weights to estimate the relative likelihood of each model given the data (Akaike 1973, Hurvich and Tsai 1989, Burnham and Anderson 2002). We summed Akaike weights across all the models containing the variable of interest to estimate the relative importance of

variables. To determine the direction and magnitude of effect sizes for variables, we calculated the mean standardized regression coefficient across all the models containing the variable of interest, and estimated precision using an unconditional variance estimator that incorporates model selection uncertainty (Burnham and Andersen 2002: 162). Using this variance estimate, we calculated 95%, 90%, and 85% confidence intervals (CI) of each coefficient and scored the magnitude of effect as "no effect" where the 85% CI spans zero, "weak effect" where the 85% CI does not span zero, "moderate effect" where the 90% CI does not span zero and "strong effect" where the 95% CI does not span zero (sensu Skagen et al. 2005). We calculated the coefficient of determination of the linear model that includes only those predictor variables exhibiting moderate or strong effects to determine the amount of variation explained.

We also analyzed general patterns in the annual variability of waterfowl populations and distributions. We obtained mean monthly precipitation data from 17 weather stations within the KDAX radar domain during December and January of each winter from NCDC. We used linear regression analysis to test for relationships of year and mean monthly precipitation (independent variables) with seasonal mean radar reflectivity, and the ratio of reflectivity at flooded rice fields relative to wetland habitats (dependent variables). We determined the mean radar reflectivity at flooded rice fields as the overall mean among all pulse volumes whose 2-dimensional extent over land was comprised primarily of flooded rice ($\geq$ 85%). We also performed linear regression of seasonal mean radar reflectivity on year at the individual pulse volume level to map where changes in bird distributions over time have occurred.

RESULTS

General Waterfowl Distribution Patterns:

Overall, we sampled evening wintering waterfowl flights from 32% (403 of 1240) of potential days (see Appendix A). We excluded the remaining 68% percent of days from analyses due to the presence of precipitation (28%), missing data in the archive (27%), or anomalous propagation of the radar beam (13%). Within sampling seasons, mean radar reflectivity (i.e., relative bird density) was variable, but exhibited a peak during week 6 (4 – 11 January) across years and radars (Figure 9). Across winters, mean radar reflectivity at KDAX varied positively in response to both year and the mean monthly precipitation (r^2 = 0.455, $F_{2,10}$ = 4.2, P = 0.05; Figure 10). Thus, waterfowl populations within the KDAX radar domain increased over time and were larger during winters with greater precipitation. Similarly, the ratio of mean radar reflectivity at flooded rice fields relative to wetlands increased positively in response to both year and the mean monthly precipitation (r^2 = 0.798, $F_{2,10}$ = 19.7, P < 0.001; Figure 11). Thus, waterfowl use of flooded rice fields relative to wetlands was greater over time and during winters with greater precipitation.

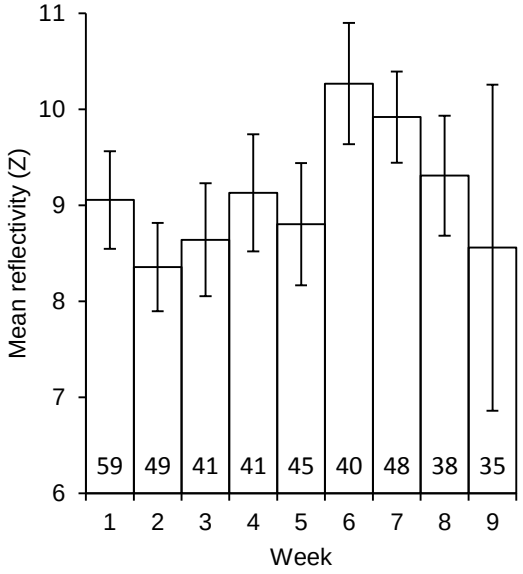

Figure 9. Mean ± SE reflectivity within radar coverage area by week across years and radars. Number of sampling days at bottom of bars.

Relative waterfowl density changed over the 13-year time period (Figure 12). Discrete areas with the strongest and most extensive trends of declining bird density were located within the Colusa, Butte, Cosumnes, Solana, and Suisin Marsh basins. These areas also exhibited strong declining trends in wetness over time. Discrete areas with the strongest and most extensive trends of increasing bird density were located within the Sutter, Colusa, and American basins. These areas coincided with areas of rice fields that experienced strong increases in wetness over time. Other discrete areas with strong increases in bird density were associated with restored wetlands in the Solano and East San Joaquin basins.

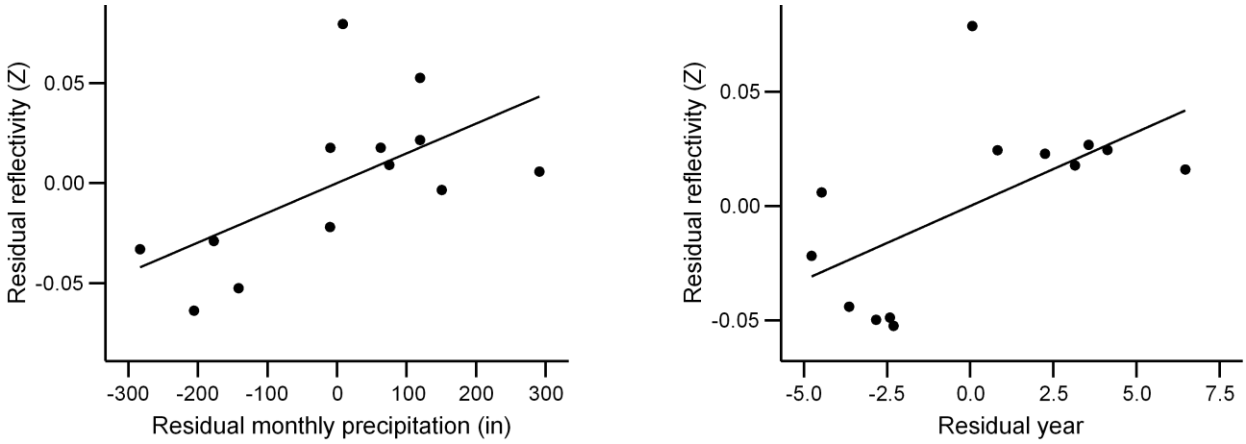

Figure 10. Partial regression plots of mean radar reflectivity at KDAX on mean monthly precipitation and year.

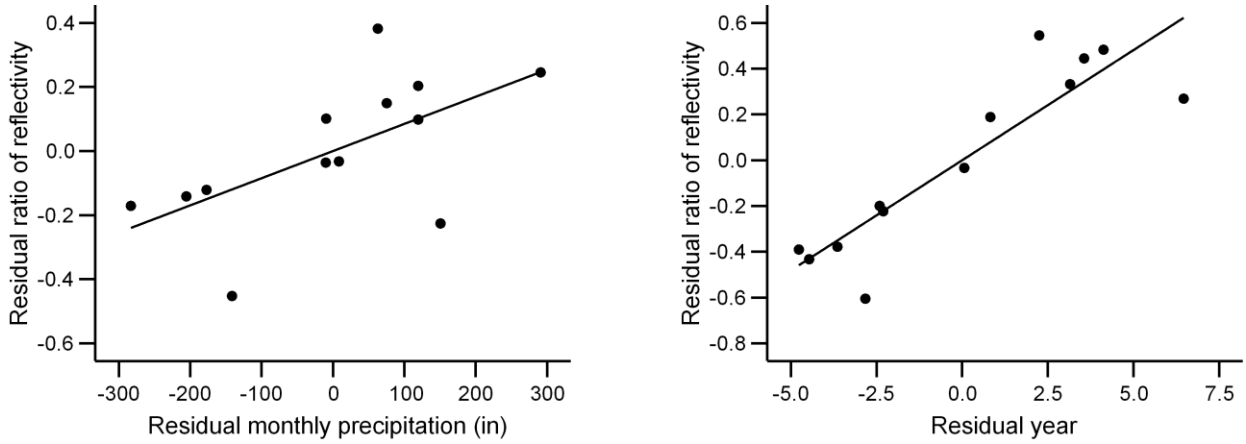

Figure 11. Partial regression plots of the ratio of mean radar reflectivity at flooded rice fields relative to wetlands at KDAX on mean monthly precipitation and year.

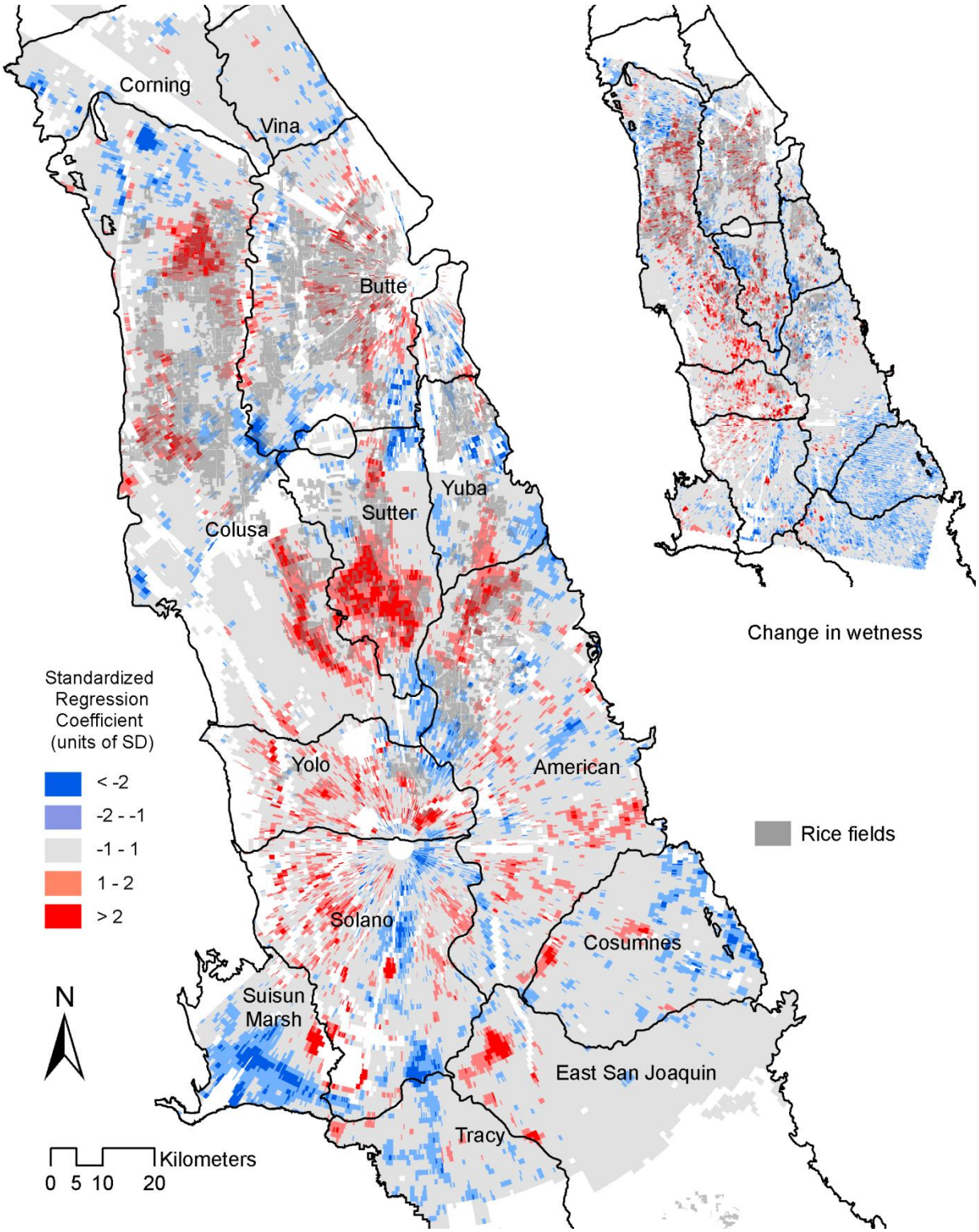

Figure 12. Map of the direction and magnitude of linear trends (i.e., standardized regression coefficients) of mean radar reflectivity and mean wetness index (inset) through time (1995 to 2007) for individual sample volumes. Boundaries and names of ground water basins and the locations of rice fields are shown for reference.

Waterfowl Use of Wetland Reserve Program Sites Before Restoration: During pre-enrollment years the overall mean standardized bird density at WRP site clusters was 1.42 ± 0.60 and not different from that at existing wetlands (t = 0.70, df =18, P = 0.49). Most of the variability (r^2 = 0.72) in bird density among sites was explained by the amount of wetland and open water area in the surrounding landscape and the mean distance from the nearest wetland (Table 2). These three variables exhibited strong effects and were positively related to bird density (Figure 13), such that bird density increased with greater wetland and open water area in the landscape and with greater distance from the nearest wetland. Effects of site characteristic on bird density during pre-enrollment years had no support.

Waterfowl Use of Wetland Reserve Program Sites After Restoration: After restoration, we detected increases in standardized bird density at most site clusters (84%) with a mean relative increase of 469 ± 94%. The overall mean standardized bird density at sites that exhibited increases was 3.79 ± 1.67 and not different from that at existing wetlands (t = 1.67, df =15, P = 0.12). Bird density at the remaining three site clusters decreased (16%) with a mean relative decrease of 39 ± 11%. We produced time series charts of the annual change in bird density and amount of winter flooding at sites at the 43 individual WRP easements that comprised the 19 site clusters (see Appendix C). The easements within the three clusters (WRP cluster 206, 309, and 310) that had greater mean bird density before restoration experienced extensive flooding during one or more pre-enrollment years that coincided with exceptionally high bird density. These events exerted a strong influence on the calculation of mean bird density values and likely explain the apparent decline in bird density after restoration.

Most of the variability (r^2 = 0.81) in bird density among sites was explained by the standardized bird density during pre-enrollment years, the amount of wetland area in the surrounding landscape, the difference in site wetness between pre-enrollment and post-restoration years, and the mean distance from the nearest flooded rice field (Table 3). All of these variables exhibited strong effects on bird density, except for distance from nearest flooded rice field (moderate effect). Sites with high baseline bird density before enrollment had high bird density after restoration. However, bird density after restoration also

increased with less wetland area in the landscape, greater increase in site wetness after restoration, and closer proximity to flooded rice fields (Figure 14).

We produced a map of predicted post-restoration standardized bird density on agricultural lands (Figure 15) using the model-averaged parameter estimates of variables important in explaining bird density and assuming no change in site wetness index after restoration with the following equation:

$$\text{Bird density}_{post} = e^{1.0632 \times \ln \text{Bird density}_{\text{pre}} + -6.1563 \times \sin^{-1} \overline{\%\text{ wetland within 1.5 km}} + -0.2716 \times \ln \text{Distance to flooded rice} + 3.1375},$$

where $\text{Bird density}_{pre}$ is the predicted mean standardized bird density during pre-enrollment years calculated using the following equation:

$$\text{Bird density}_{pre} = e^{6.8965 \times \sin^{-1} \overline{\%\text{ wetland within 2 km}} + 0.9143 \times \ln \text{Distance to wetland} + 2.563 \times \sin^{-1} \overline{\%\text{ water within 0.5 km}} - 7.7401}.$$

We used land cover from 1999 and surface water data from 5 February 1999 to model bird density.

Table 2. Importance and effect size of variables in explaining standardized bird density (ratio of reflectivity relative to that of wetland habitats) during **pre-enrollment** years among WRP site clusters. Effect size is the standardized regression coefficient for each variable averaged across all models ± unconditional SE. See Appendix B for summary statistics of explanatory variables.

Variable type	Explanatory variable	Effect size	Relative importance
Site characteristic	Site area	0.11 ± 0.20	0.15
	Site wetness index	0.23 ± 0.20	0.25
Landscape placement	Distance from wetland	**0.55 ± 0.18*** **	0.92
	Distance from flooded rice field	0.25 ± 0.22	0.28
Landscape composition	Wetland within 2.0 km	**0.70 ± 0.21*** **	0.96
	Flooded rice within 0.5 km	-0.27 ± 0.22	0.31
	Open water within 0.5 km	**0.41 ± 0.20*** **	0.66

*** Strong effect, ** Moderate effect, * Weak effect

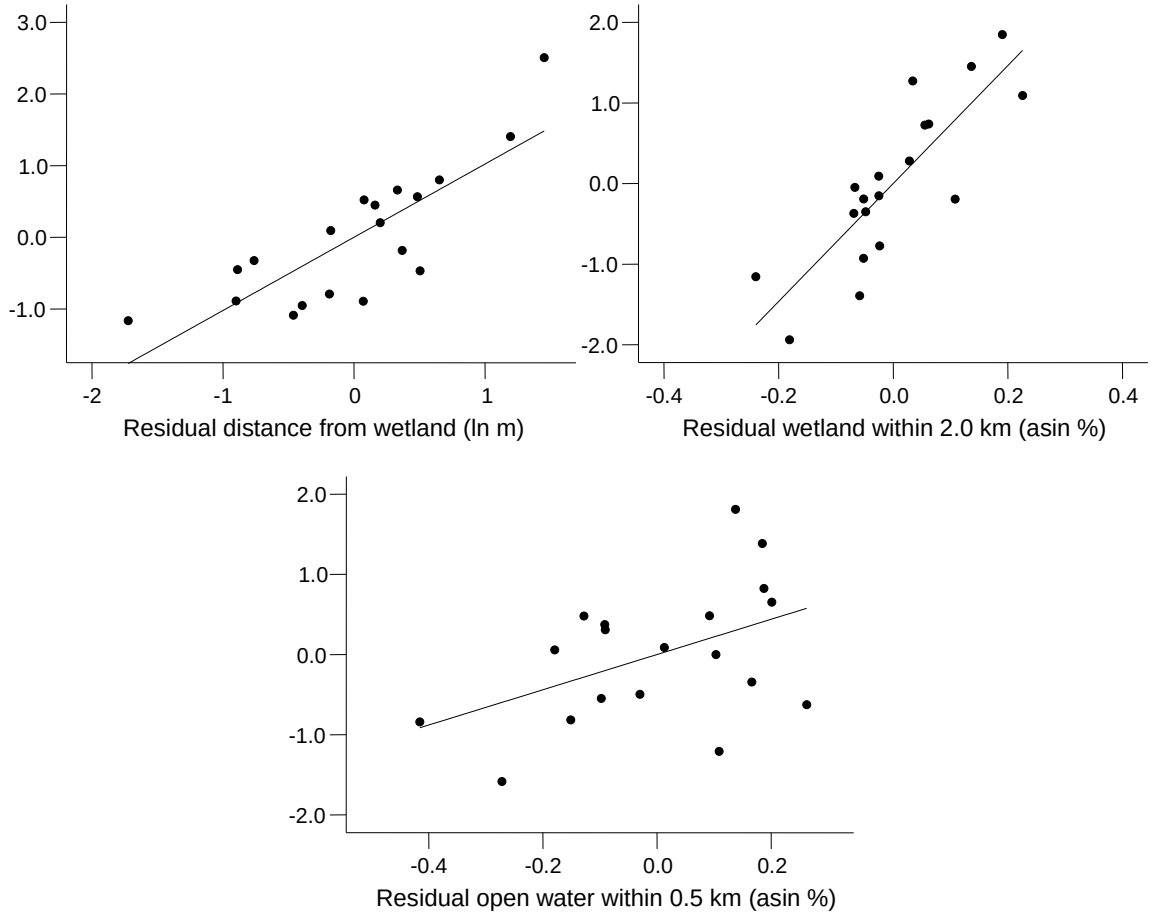

Figure 13. Series of partial regression plots from linear model of explanatory variables (x-axes) that exhibit effects in explaining standardized bird density (ratio of reflectivity relative to that of wetland habitats) during pre-enrollment years (y-axis; residual values log-transformed).

Table 3. Importance and effect size of variables in explaining standardized bird density (ratio of reflectivity relative to that of wetland habitats) during **post-restoration** years among WRP site clusters. Effect size is the standardized regression coefficient for each variable averaged across all models ± unconditional SE. See Appendix B for summary statistics of explanatory variables.

Variable type	Explanatory variable	Effect size	Relative importance
Site characteristic	Pre-enrollment bird density	**1.11 ± 0.21*** **	1.00
	Restored wetland area	0.09 ± 0.17	0.13
	Change in wetness index	**0.40 ± 0.14*** **	0.91
	Mean age of restoration	0.05 ± 0.15	0.11
Landscape placement	Distance from wetland	-0.24 ± 0.23	0.24
	Distance from flooded rice field	**-0.32 ± 0.17** **	0.51
Landscape composition	Wetland within 1.5 km	**-0.62 ± 0.21*** **	0.96
	Flooded rice within 1.0 km	0.18 ± 0.20	0.22
	Open water within 0.5 km	-0.02 ± 0.25	0.14

*** Strong effect, ** Moderate effect, *Weak effect

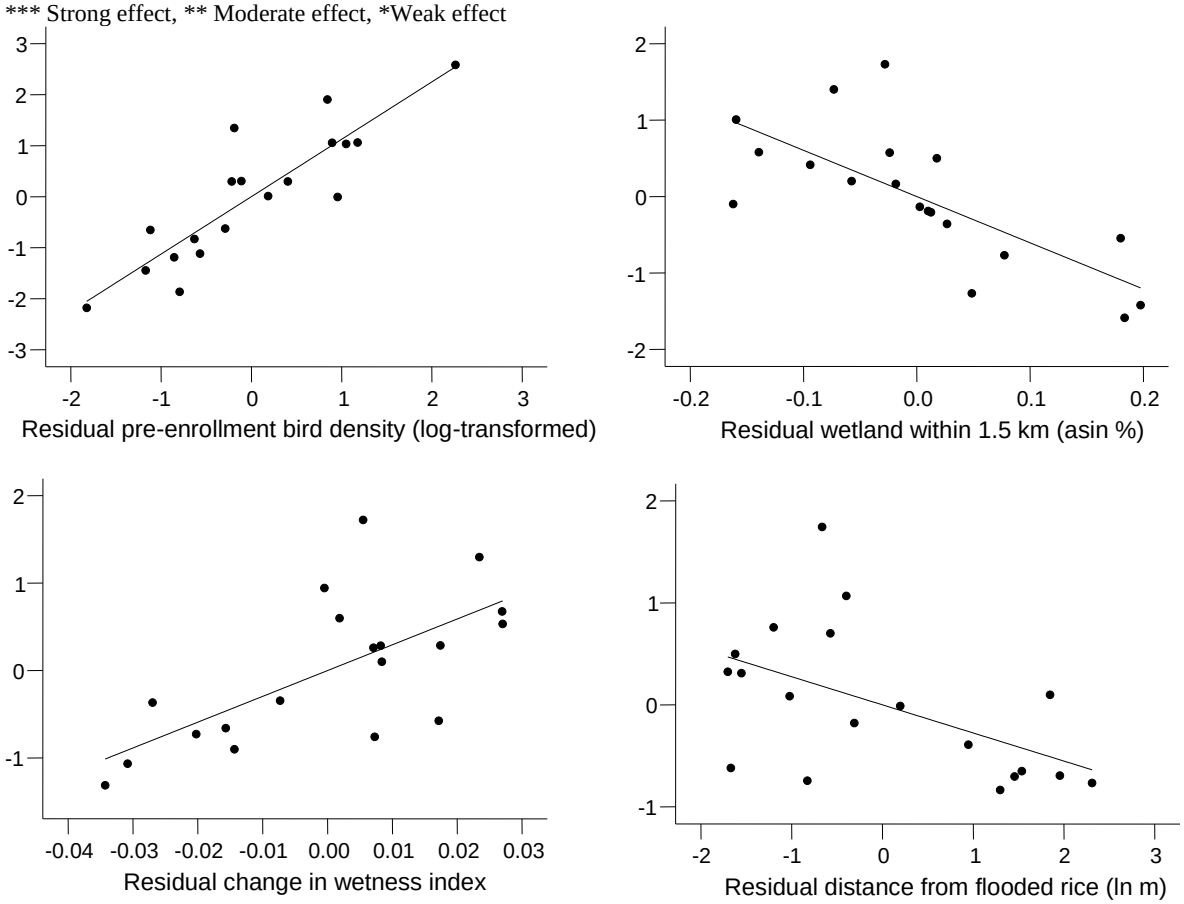

Figure 14. Series of partial regression plots from linear model of explanatory variables (x-axes) that exhibit effects in explaining standardized bird density (ratio of reflectivity relative to that of wetland habitats) during post-enrollment years (y-axis; residual values log-transformed).

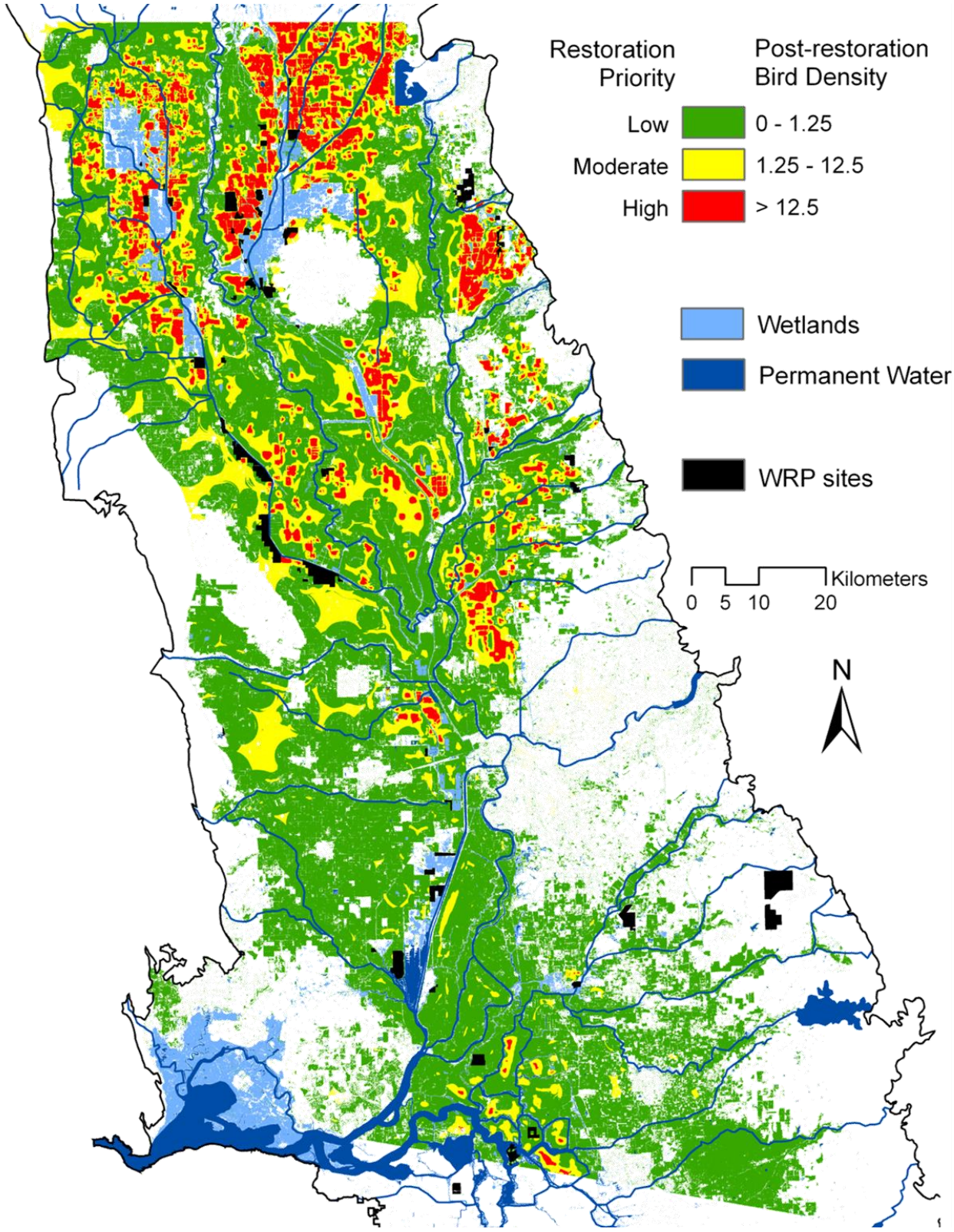

Figure 15. Map of predicted post-restoration standardized bird density (ratio of reflectivity relative to that of wetland habitats) and associated potential wetland restoration priority category on agricultural lands within the northern Central Valley of California based on 1999 land cover and winter surface water.

DISCUSSION

Waterfowl Use of Wetland Reserve Program Sites Before Restoration: Because WRP sites are active agricultural fields before enrollment, we expected limited diurnal use by roosting waterfowl at these sites. This is because mallards and northern pintails are more likely to occur in wetlands than agricultural fields during the day in the CVC (J. Fleskes, personal communication). However, waterfowl use at sites during pre-enrollment years was, on average, unexpectedly high by being similar to that at existing wetlands. This result is likely indicative of "contamination" in radar measures of the airspace over sites caused by waterfowl dispersing from adjacent wetlands in the local landscape. Thus, the magnitude of waterfowl use before restoration likely represents bias in radar measures reflecting general waterfowl abundance in the local landscape.

The use of wetlands by waterfowl and other wetland-dependent birds is positively related to the amount of wetlands and/or open water in the local landscape (Brown and Dinsmore 1986, Fairbairn and Dinsmore 2001, McKinstry and Anderson 2002, Taft and Haig 2006, Stafford et al. 2007, Anteau and Afton 2009, Webb et al. 2010). Accordingly, we found that WRP sites in landscapes with more wetland and open water habitat had greater relative bird density during pre-enrollment years. Webb et al. (2010) hypothesize that landscape-scale complexes of wetlands contain a variety of different wetland types, which provide dabbling ducks with a greater diversity of food items compared to isolated wetlands. This is consistent with the resource concentration hypothesis, which postulates that individuals should concentrate disproportionately in areas of high resource abundance, and because larger patches often contain greater abundance of resources, density is predicted to correlate positively with patch area (Connor et al. 2000). Additionally, most wetlands in the CVC are within managed wetland complexes that may also serve as daytime roost sites for ducks that engage in nocturnal foraging flights into the surrounding landscape as an adaptation to disturbance during the day (Cox and Afton 1997).

We found that sites immediately adjacent to wetlands had relatively lower pre-enrollment bird density than sites that were up to 1 km from a nearby wetland when controlling for the effects of the amount of wetlands and/or open water in the local landscape. This likely reflects a biological impact of

the relative isolation of WRP sites on waterfowl use rather than a measurement bias of the radar. Because waterfowl are gregarious during the winter (Paulus 1988) and agricultural fields are less suitable to wetlands for roosting waterfowl, the more isolated WRP sites may have a greater propensity to be used and concentrate flocks of birds than sites adjacent to wetlands where birds are more likely to use the neighboring wetland habitat first *sensu* ideal free distribution theory (Fretwell and Lucas 1970).

Waterfowl Use of Wetland Reserve Program Sites After Restoration: Weather surveillance radars detected increased daytime use by waterfowl at nearly all WRP sites after wetland restoration. However, the magnitude of the response to restoration by waterfowl varied considerably among sites and was closely related to the amount of surrounding wetland habitat in the local landscape, site wetness (hydrology), the proximity of the site to flooded rice fields, and, most importantly, to pre-enrollment bird density. By treating pre-enrollment bird density as a control for measurement bias due to contamination caused by birds dispersing from the surrounding landscape, the biological interpretations of the remaining factors influencing the response of waterfowl to restoration at WRP sites are clearer.

After pre-enrollment bird density, the amount of surrounding wetland habitat in the local landscape had the greatest relative effect on the response of waterfowl to restoration. Surprisingly, this relationship was negative, indicating that post-restoration bird density decreased with increasing wetland habitat in the landscape. This contradicts the prevailing theory that waterfowl use of restored wetlands should be positively related to the amount of wetlands in the local landscape, which is based on evidence from waterfowl use of natural wetlands (Brown and Dinsmore 1986, Fairbairn and Dinsmore 2001, McKinstry and Anderson 2002, Stafford et al. 2007, Webb et al. 2010). However, ours is the first study that we are aware of that explicitly tests this relationship for restored wetlands. These results suggest that restored wetlands are used relatively less by waterfowl in landscapes where other wetlands are abundant despite the overall similarity of waterfowl densities between restored and other wetlands. Although Ratti et al. (2001) found that densities of breeding waterfowl were also similar between restored and natural wetlands, Brown and Smith (1998) found that breeding waterfowl densities were lower at restored wetlands relative to natural wetlands even after 3 growing seasons. Thus, restored wetlands may not be

ecologically equivalent to natural wetlands. Whether this is true for WRP sites in the CVC is currently under investigation (W. Duffy, personal communication).

For restored wetlands, typical wetland conditions and processes can develop quickly (e.g., within a year) and aquatic and terrestrial productivity can be similar to that of natural wetlands (McKenna 2003). However, because wetland restoration typically relies on natural colonization, successional progress can be slow and the biotic community structure of restored wetlands usually comprises a subset of species found in natural wetlands and maintains productivity through different food web pathways (Galatowitsch and van der Valk 1996, McKenna 2003, Seabloom and van der Valk 2003). For example, aquatic macroinvertebrate communities in CVC restored wetlands may take 5 to 10 years before resembling those of natural wetlands (Marchetti et al. 2010). Additionally, one of the most persistent differences between restored and natural wetlands is the absence of woody vegetation at restored sites (Brown and Smith 1998). How these biotic community differences influence waterfowl use is unclear and beyond the scope of this study. We encourage future research to corroborate our results and to investigate how/why restored wetlands may be less suitable for waterfowl in landscapes where natural wetlands are abundant.

Most of the WRPs in the CVC are under some degree of active moist soil management, defined as the manipulation of water levels to mimic natural hydrology and stimulate production of plants and invertebrates that provide food for wintering waterfowl and other wetland wildlife (Baldassarre and Bolen 2006). Not surprisingly, we found the intensity of moist soil management had an important effect on wintering waterfowl response, as others have found for waterbirds during spring and summer (Kaminski et al. 2006, O'Neal et al. 2008). WRP sites with the greatest increases in site soil wetness after restoration had the greatest post-restoration waterfowl use. Thus active restoration of hydrology and intensity of moist-soil management is important for maximizing the benefit of WRP sites for supporting wintering waterfowl.

The proximity of WRP sites to flooded rice fields also influenced post-restoration waterfowl use. Rice fields, particularly flooded rice fields, are an important habitat used by feeding waterfowl within the CVC. In fact, waterfowl have shifted their distributions over time to track the increase in flooded rice area

(Fleskes et al. 2005b, Ackerman et al. 2006). So, it is not surprising that we found waterfowl use was relatively greater at sites closer to flooded rice.

General Waterfowl Distribution Patterns: Our analysis of the 13-year radar data archive revealed several aspects of the spatio-temporal dynamics of waterfowl population and distribution patterns that corroborate important findings by others while also providing new information. This provides further support for the utility of weather surveillance radars for observing and quantifying waterfowl distributions beyond the direct ground-truthing that we performed for Objective 1. Additionally, some of these general distribution patterns should be taken into consideration when evaluating future WRP enrollment strategies.

For example, we found waterfowl use of flooded rice fields as roosting habitat nearly tripled from 1995 to 2007 relative to waterfowl use of wetlands. This corroborates previous radio-telemetry studies that documented similar shifts in winter roosting use of agricultural habitats relative to wetland habitats during the 1990's for white-fronted geese, northern pintails, and mallards (Fleskes et al. 2005b, Ackerman et al. 2006). However, unlike the telemetry data which measured habitat use at just two time periods, radar observations provided annual measures. This revealed that habitat use is also dependent upon the amount of precipitation, such that wetlands were used more heavily during drier years. Furthermore, we were able to document annual changes in overall waterfowl populations that positively tracked the amount of precipitation and also exhibited an increasing trend over time. Mid-winter aerial surveys conducted by California Department of Fish and Game and U.S. Fish and Wildlife Service also exhibit an increasing trend over time.

As mentioned earlier, shifts in habitat use have been accompanied by region-wide shifts in the general distributions of waterfowl within the CVC that are positively related to increases in the amount of rice production, flooded rice, and wetland habitat within basins. Specifically, distributions of white-fronted geese increased within the American Basin and the Sutter National Wildlife Refuge within the Sutter Basin between 1987-1990 and 1998-2000 (Ackerman et al. 2006). Our radar analysis revealed these same shifts in waterfowl distributions and provided a more comprehensive and spatially-explicit

view of where distributional changes occurred within the northern CVC during the past 15 years. This information should be considered for future WRP enrollments by targeting regions in the CVC that are experiencing increasing waterfowl use and not in regions where waterfowl use is declining. We were unable to associate spatially-explicit changes in waterfowl distributions to spatially-explicit changes in land cover because we did not have suitable land cover data available for quantifying change.

Although not the focus of this study, the peak of wintering waterfowl density observed by the radars coincided with the peak in waterfowl numbers based on aerial surveys (Fleskes et al. 2005b). Additionally, we found regional shifts in bird distributions within winters that also coincided with similar regional shifts documented by aerial surveys. Thus, radar observations could be used to answer questions related to daily distributional patterns and activity of waterfowl in relation to hunting pressure, changes in surface water availability, and weather events.

Conclusions and Management Implications: WRP sites provide habitat for wintering waterfowl within the CVC. Waterfowl dramatically increase and maintain their use of WRP sites over an average of 3 years starting the first winter after the restoration of hydrology. Maximizing waterfowl use of WRP sites can be achieved by locating sites close to flooded rice fields within local landscapes with high general waterfowl abundance and relatively little existing wetland area and by intensively managing moist-soil at the site. We developed a map as a decision support tool for prioritizing future WRP enrollments that predicts the post-restoration magnitude of waterfowl use based on the site and local landscape variables associated with relative waterfowl use. Additionally, changes in waterfowl distributions during the past 15 years and the increasing importance of flooded rice for waterfowl should be considered for future WRP enrollment strategies.

ACKNOWLEDGEMENTS

We thank Joe Fleskes at the USGS Western Ecological Research Center for waterfowl radio telemetry and land cover data and helpful discussions of waterfowl biology, Jessica Groves at NRCS in California for logistical support and WRP site data, Tianna Bogart and Daria Kluver at the University of Delaware for software development, and Robert Diehl at the University of Southern Mississippi for

helpful discussions of radar data processing methods. Telemetry data used in our analysis were the result of efforts of numerous individuals and organizations as described in Fleskes et al. (2005b). Any use of trade, product, or firm names is for descriptive purposes only and does not imply endorsement by the U.S. Government.

REFERENCES

Ackerman, J. T., J. Y. Takekawa, D. L. Orthmeyer, J. P. Fleskes, J. L. Yee, and K. L. Kruse. 2006. Spatial use by wintering Greater White-fronted Geese relative to a decade of habitat change in California's Central Valley. Journal of Wildlife Management 70:965-976.

Akaike, H. 1973. Information theory as an extension of the maximum liklihood principle. Pages 267-281 *in* Second International Symposium on Information Theory. Akademiai Kiado, Budapest.

Åkesson, S., T. Alerstam, and A. Hedenström. 1996. Flight initiation of nocturnal passerine migrants in relation to celestial orientation conditions at twilight. Journal of Avian Biology 27:95-102.

Alsdorf, D. E., E. Rodriguez, and D. P. Lettenmaier. 2007. Measuring surface water from space. Reviews of Geophysics 45. doi: 10.1029/2006RG000197.

Andrieu, H., and J. D. Creutin. 1995. Identification of vertical profiles of radar reflectivity for hydrological applications using an inverse method. Part I: Formulation. Journal of Applied Meteorology 34:225-239.

Anteau, M. J., and A. D. Afton. 2009. Wetland use and feeding by Lesser Scaup during spring migration across the Upper Midwest, USA. Wetlands 29:704-712. doi: 10.1672/08-157.1.

Baldassarre, G. A., and E. G. Bolen. 1984. Field-feeding ecology of waterfowl wintering on the southern high plains of Texas. The Journal of Wildlife Management 48:63-71.

Baldassarre, G. A., and E. G. Bolen. 2006. Waterfowl Ecology and Management, 2nd edition. Kreiger Publishing Co., Malabar, FL.

Bonter, D. N., S. A. Gauthreaux, and T. M. Donovan. 2009. Characteristics of important stopover locations for migrating birds: Remote sensing with radar in the Great Lakes Basin. Conservation Biology 23:440-448.

Brown, M., and J. J. Dinsmore. 1986. Implications of marsh size and isolation for marsh bird management. The Journal of Wildlife Management 50:392-397.

Brown, S. C., and C. R. Smith. 1998. Breeding season bird use of recently restored versus natural wetlands in New York. The Journal of Wildlife Management 62:1480-1491.

Buler, J. J., and R. H. Diehl. 2009. Quantifying bird density during migratory stopover using weather surveillance radar. IEEE Transactions on Geoscience and Remote Sensing 47:2741-2751. doi: 10.1109/TGRS.2009.2014463.

Burnham, K. P., and D. R. Anderson. 2002. Model Selection and Multimodel Inference: A Practical Information-Theoretic Approach. 2nd ed. Springer, New York.

Connor, E. F., A. C. Courtney, and J. M. Yoder. 2000. Individuals-area relationships: the relationship between animal population density and area. Ecology 81:734-748.

Cox, R. R., and A. D. Afton. 1996. Evening flights of female Northern Pintails from a major roost site. The Condor 98:810-819.

Cox, R. R., and A. D. Afton. 1997. Use of habitats by female northern pintails wintering in southwestern Louisiana. The Journal of Wildlife Management 61:435-443.
Cressie, N. A. C. 1993. Statistics for spatial data. Wiley, New York.
Crist, E. P. 1985. A TM Tasseled Cap equivalent transformation for reflectance factor data. Remote Sensing of Environment 17:301-306. doi: 10.1016/0034-4257(85)90102-6.
Crist, E. P., and R. C. Cicone. 1984. A physically-based transformation of Thematic Mapper data---The TM Tasseled Cap. IEEE Transactions on Geoscience and Remote Sensing GE-22:256-263. doi: 10.1109/TGRS.1984.350619.
Crum, T. D., and R. L. Alberty. 1993. The WSR-88D and the WSR-88D operational support facility. Bulletin of the American Meteorological Society 74:1669-1687.
Diehl, R. H., and R. P. Larkin. 2005. Introduction to the WSR-88D (NEXRAD) for ornithological research. Pages 876-888 *in* C. J. Ralph and T. D. Rich, editors. Bird Conservation Implementation and Integration in the Americas: Proceedings of the Third International Partners in Flight Conference 2002 March 20-24. Pacific Southwest Research Station, Forest Service, U.S.D.A., Gen. Tech. Rep. PSW-191, Albany, CA, Asilomar, California.
Diehl, R. H., R. P. Larkin, and J. E. Black. 2003. Radar observations of bird migration over the Great Lakes. The Auk 120:278-290.
Ely, C. R. 1992. Time allocation by Greater White-fronted Geese: Influence of diet, energy reserves and predation. The Condor 94:857-870.
Fairbairn, S. E., and J. J. Dinsmore. 2001. Local and landscape-level influences on wetland bird communities of the prairie pothole region of Iowa, USA. Wetlands 21:41-47.
Fleskes, J. P., W. M. Perry, K. L. Petrik, R. Spell, and F. Reid. 2005a. Change in area of winter-flooded and dry rice in the northern Central Valley of California determined by satellite imagery. California Fish and Game 91:207-215.
Fleskes, J. P., J. L. Yee, M. L. Casazza, M. R. Miller, J. Y. Takekawa, and D. L. Orthmeyer. 2005b. Waterfowl distribution, movements, and habitat use relative to recent habitat changes in the Central Valley of California: A cooperative project to investigate impacts of the Central Valley Joint Venture and changing agricultural practices on the ecology of wintering waterfowl. Final Report. U.S. Geological Survey - Western Ecological Research Center, Dixon Field Station, Dixon, CA.
Fleskes, J. P., R. L. Jarvis, and D. S. Gilmer. 2002. Distribution and movements of female Northern Pintails radiotagged in San Joaquin Valley, California. The Journal of Wildlife Management 66:138-152.
Fretwell, S. W., and H. L. Lucas. 1970. On territorial behavior and other factors influencing habitat distribution in birds. I. Theoretical development. Acta Biotheoretica 19:16-36.
Galatowitsch, S. M., and A. G. van der Valk. 1996. The vegetation of restored and natural prairie wetlands. Ecological Applications 6:102-112.
Gauthreaux, S. A., and C. G. Belser. 1998. Displays of bird movements on the WSR-88D: patterns and quantification. Weather and Forecasting 13:453-464.
Gauthreaux, S. A., and C. G. Belser. 2003. Radar ornithology and biological conservation. The Auk 120:266-277.
Gauthreaux, S. A., C. G. Belser, and D. V. Blaricom. 2003. Using a network of WSR-88D weather surveillance radars to define patterns of bird migration at large spatial scales. Pages 335-346 *in* P. Berthold, E. Gwinner, and E. Sonnenschein, editors. Avian migration. Springer-Verlag, Germany.

Gauthreaux, S. A. 1971. A radar and direct visual study of passerine spring migration in southern Louisiana. The Auk 88:343-365.
Hebrard, J. J. 1971. The nightly initiation of passerine migration in spring: A direct visual study. Ibis 113:8-18.
Hedenström, A., and T. Alerstam. 1992. Climbing performance of migrating birds as a basis for estimating limits for fuel-carrying capacity and muscle work. Journal of Experimental Biology 164:19-38.
Holland, J. D., D. G. Bert, and L. Fahrig. 2004. Determining the spatial scale of species' response to habitat. Bioscience 54:227-233.
Huang, C., B. Wylie, L. Yang, C. Homer, and G. Zylstra. 2002. Derivation of a tasselled cap transformation based on Landsat 7 at-satellite reflectance. International Journal of Remote Sensing 23:1741-1748.
Hurvich, C. M., and C. Tsai. 1989. Regression and time series model selection in small samples. Biometrika 76:297-307.
Johnson, F. A., K. H. Pollock, and F. Montalbano III. 1989. Visibility bias in aerial surveys of Mottled Ducks. Wildlife Society Bulletin 17:222-227.
Kaminski, M. R., G. A. Baldassarre, and A. T. Pearse. 2006. Waterbird responses to hydrological management of Wetlands Reserve Program habitats in New York. Wildlife Society Bulletin 34:921-926.
Marchetti, M. P., M. Garr, and A. N. H. Smith. 2010. Evaluating wetland restoration success using aquatic macroinvertebrate assemblages in the Sacramento Valley, California. Restoration Ecology 18:457-466. doi: 10.1111/j.1526-100X.2008.00468.x.
Mausbach, M. J., and A. R. Dedrick. 2004. The length we go: measuring environmental benefits of conservation practices. Journal of Soil and Water Conservation 59:97A-103A.
McKenna, J. 2003. Community metabolism during early development of a restored wetland. Wetlands 23:35-50. doi: 10.1672/0277-5212(2003)023[0035:CMDEDO]2.0.CO;2.
McKinstry, M. C., and S. H. Anderson. 2002. Creating wetlands for waterfowl in Wyoming. Ecological Engineering 18:293-304. doi: 10.1016/S0925-8574(01)00088-X.
Miller, M. R. 1985. Time budgets of Northern Pintails wintering in the Sacramento Valley, California. Wildfowl 36:53-64.
Miller, M. R., J. Y. Takekawa, J. P. Fleskes, D. L. Orthmeyer, M. L. Casazza, and W. M. Perry. 2005. Spring migration of Northern Pintails from California's Central Valley wintering area tracked with satellite telemetry: routes, timing, and destinations. Canadian Journal of Zoology 83:1314-1332.
O'Neal, B. J., E. J. Heske, and J. D. Stafford. 2008. Waterbird response to wetlands restored through the Conservation Reserve Enhancement Program. Journal of Wildlife Management 72:654-664.
O'Neal, B. J., J. D. Stafford, and R. P. Larkin. 2010. Waterfowl on weather radar: applying ground-truth to classify and quantify bird movements. Journal of Field Ornithology 81:71-82.
Orians, G. H. 1961. The ecology of blackbird (Agelaius) social systems. Ecological Monographs 31:285-312.
Paulus, S. L. 1988. Time-activity budgets of nonbreeding Anatidea: A review. Pages 135-152 *in* M. W. Weller, editor. Waterfowl in winter. Minnesota Press, Minneapolis.
Pollock, K. H., and W. L. Kendall. 1987. Visibility bias in aerial surveys: A review of estimation procedures. The Journal of Wildlife Management 51:502-510.

Ratti, J. T., A. M. Rocklage, J. H. Giudice, E. O. Garton, and D. P. Golner. 2001. Comparison of avian communities on restored and natural wetlands in North and South Dakota. The Journal of Wildlife Management 65:676-684.

Raveling, D. G., W. E. Crews, and W. D. Klimstra. 1972. Activity patterns of Canada Geese during winter. Wilson Bulletin 84:278-295.

Rewa, C. A. 2005. Wildlife benefits of the Wetlands Reserve Program. Pages 133-145 *in* Fish and wildlife benefits of Farm Bill conservation programs: 2000-2005 update. The Wildlife Society Technical Review 05-2, Bethesda, MD.

Russell, K. R., D. S. Mizrahi, and S. A. Gauthreaux. 1998. Large-scale mapping of purple martin pre-migratory roosts using WSR-88D weather surveillance radar. Journal of Field Ornithology 69:316-325.

Ruth, J. M., J. J. Buler, R. H. Diehl, and R. S. Sojda. 2008. Management and research applications of long-range surveillance radar data for birds, bats, and flying insects. U.S. Geological Survey, Fact Sheet 2008-3095. Retrieved from http://pubs.usgs.gov/fs/2008/3095/pdf/FS08-3095_508.pdf.

Seabloom, E., and A. van der Valk. 2003. Plant diversity, composition, and invasion of restored and natural prairie pothole wetlands: Implications for restoration. Wetlands 23:1-12. doi: 10.1672/0277-5212(2003)023[0001:PDCAIO]2.0.CO;2.

Seibert, H. C. 1951. Light intensity and the roosting flight of herons in New Jersey. The Auk 68:63-74.

Silverman, B. W. 1986. Density estimation for statistics and data analysis. Chapman and Hall, London.

Skagen, S. K., J. Kelly, C. van Riper III, R. L. Hutto, D. Finch, D. J. Krueper, and C. P. Melcher. 2005. Geography of spring landbird migration through riparian habitats in southwestern North America. Condor 107:212-227.

Smith, L. C. 1997. Satellite remote sensing of river inundation area, stage, and discharge: a review. Hydrological Processes 11:1427-1439.

Stafford, J. D., M. M. Horath, A. P. Yetter, C. S. Hine, and S. P. Havera. 2007. Wetland use by Mallards during spring and fall in the Illinois and Central Mississippi River Valleys. Waterbirds 30:394-402. doi: doi: 10.1675/1524-4695(2007)030[0394:WUBMDS]2.0.CO;2.

Stevens, C. E., T. S. Gabor, and A. W. Diamond. 2003. Use of restored small wetlands by breeding waterfowl in Prince Edward Island, Canada. Restoration Ecology 11:3-12.

Taft, O., and S. Haig. 2006. Importance of Wetland Landscape Structure to Shorebirds Wintering in an Agricultural Valley. Landscape Ecology 21:169-184. doi: 10.1007/s10980-005-0146-5.

Tamisier, A. 1976. Diurnal activities of Green-winged Teal and Pintail wintering in Louisiana. Wildfowl 27:19-32.

Thompson, W. L. 2002. Towards reliable bird surveys: Accounting for individuals present but not detected. The Auk 119:18-25.

U.S. Fish and Wildlife Service. 1978. Concept plan for waterfowl wintering habitat and preservation, Central Valley, California. U.S. Fish and Wildlife Service, Portland, Oregon.

Warnock, S. E., and J. Y. Takekawa. 1995. Habitat preferences of wintering shorebirds in a temporally changing environment: Western Sandpipers in the San Francisco Bay estuary. The Auk 112:920-930.

Webb, E. B., L. M. Smith, M. P. Vrtiska, and T. G. Lagrange. 2010. Effects of local and landscape variables on wetland bird habitat use during migration through the Rainwater Basin. Journal of Wildlife Management 74:109-119. doi: 10.2193/2008-577.

Appendix A. Dates of radar samples for quantifying bird distributions by radar station and year. Total number of samples for each year reported in bold. Arrows indicate inclusive dates.

Radar	Year												
	1995	1996	1997	1998	1999	2000	2001	2002	2003	2004	2005	2006	2007
KDAX	**19**	**10**	**14**	**18**	**27**	**25**	**13**	**21**	**28**	**17**	**22**	**41**	**29**
	12/07	12/15	11/30	12/04	12/01	11/30	11/17	12/01	12/05	11/30	12/02	12/01	11/30
	12/08	12/16	12/01	12/09	12/02	↓	11/20	↓	12/08	↓	↓	↓	12/01
	12/16	12/24	12/09	12/10	12/04	12/04	11/21	12/05	12/11	12/02	12/06	12/07	12/04
	12/17	01/08	12/11	12/15	↓	12/07	11/27	12/07	12/15	12/04	12/08	12/10	12/05
	12/20	01/09	12/15	↓	12/08	12/08	11/28	12/08	12/16	12/05	12/12	12/16	12/08
	12/21	01/16	12/19	12/17	12/10	12/10	12/06	12/11	12/21	12/13	↓	↓	↓
	12/23	01/17	12/25	12/19	12/11	12/12	↓	12/18	12/22	↓	12/14	12/20	12/15
	↓	01/19	12/27	12/21	12/13	12/15	12/11	12/23	12/26	12/15	12/24	12/22	12/22
	12/25	01/23	12/29	12/22	↓	12/16	12/17	12/31	12/27	01/06	01/04	12/24	↓
	01/01	01/30	01/05	12/28	12/15	12/18	12/31	01/02	12/30	01/11	01/06	12/27	12/24
	↓		01/22	↓	12/17	↓		01/03	01/03	↓	01/08	↓	12/26
	01/08		01/24	12/31	12/18	12/20		01/06	01/08	01/14	01/09	01/02	12/28
	01/25		01/27	01/12	12/23	12/22		01/14	01/10	01/16	01/11	01/05	12/30
	01/28		01/30	01/13	12/24	12/24		01/15	01/11	01/29	01/12	↓	↓
				01/27	12/26	↓		01/25	01/15	↓	01/15	01/10	01/02
				↓	↓	12/27		↓	↓	01/31	01/16	01/12	01/07
				01/29	12/30	12/29		01/28	01/18		01/19	↓	01/11
					01/02	12/30		01/30	01/20		01/21	01/16	↓
					↓	01/01			↓		01/25	01/18	01/13
					01/04	01/04			01/22		01/27	↓	01/15
					01/06	01/06			01/24			01/25	01/17
					01/08	01/12			01/25				↓
					01/26				01/28				01/19
									↓				
									01/31				
KBBX	**0**	**7**	**6**	**10**	**0**	**0**	**0**	**0**	**0**	**8**	**22**	**41**	**25**
		12/02	12/31	12/08						12/21	12/03	12/01	11/30
		12/13	01/07	12/14						12/24	↓	↓	12/01
		01/08	01/20	12/19						01/06	12/06	12/07	12/08
		↓	01/22	12/24						01/13	12/08	12/15	↓
		01/10	01/27	12/27						01/16	↓	12/17	12/15
		01/15	01/30	12/30						01/20	12/10	↓	12/23
		01/17		01/01						01/29	12/12	12/19	12/24
				01/21						01/30	↓	12/22	12/26
				01/28							12/15	12/23	12/30
				01/29							01/04	12/27	12/31

Appendix A. (continued)

Radar	Year												
	1995	1996	1997	1998	1999	2000	2001	2002	2003	2004	2005	2006	2007
KBBX											01/06	↓	01/02
											01/08	01/02	01/12
											01/11	01/05	↓
											01/12	↓	01/19
											01/15	01/10	01/30
											01/19	01/12	
											01/21	↓	
											01/22	01/15	
											01/24	01/17	
											01/27	↓	
												01/25	
												01/30	
												01/31	

Appendix B. Summary statistics for explanatory variables used for modeling variation of bird density during pre-enrollment and post-restoration years among Wetland Reserve Program site clusters (n = 19).

Explanatory variable			Mean ± SD	Minimum	Maximum
Time period	Type	Name			
Pre-enrollment	Site characteristic	Site area (ha)	253 ± 362	22	1,645
		Site wetness index	-0.028 ± 0.023	-0.073	0.0144
	Landscape placement	Distance from wetland (m)	294 ± 255	35	1,012
		Distance from flooded rice field (m)	4,026 ± 5,553	50	17,122
	Landscape composition	Wetland within 2.0 km (%)	6.2 ± 7.0	0.0	22.1
		Flooded rice within 0.5 km (%)	11.5 ±15.4	0.0	44.7
		Open water within 0.5 km (%)	32.2 ±18.6	0.0	64.8
Post-restoration	Site characteristic	Pre-enrollment bird density	0.79 ± 1.04	0.02	4.57
		Restored wetland area (ha)	218 ± 302	12	1,344
		Change in wetness index	0.004 ± 0.020	-0.033	0.039
		Mean age of restoration (years)	2.9 ± 1.3	1.0	4.6
	Landscape placement	Distance from wetland (m)	263 ± 225	7	1,012
		Distance from flooded rice field (m)	3,276 ± 4,276	85	13,147
	Landscape composition	Wetland within 1.5 km (%)	5.7 ± 7.0	0.0	22.3
		Flooded rice within 1.0 km (%)	13.4 ±17.5	0.0	54.9
		Open water within 0.5 km (%)	29.1 ±18.8	0.0	64.4

Appendix C. Annual variability in mean standardized bird density (bars) and the proportion of winter flooding (line) at WRP sites. Sites identified by cluster, agreement number, and size. Bar color denotes restoration status; white = pre-enrollment, light grey = enrolled, dark grey = post-restoration.

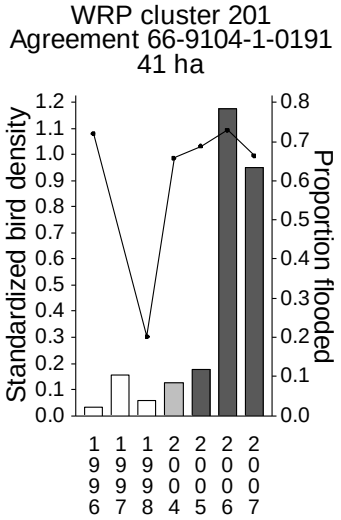

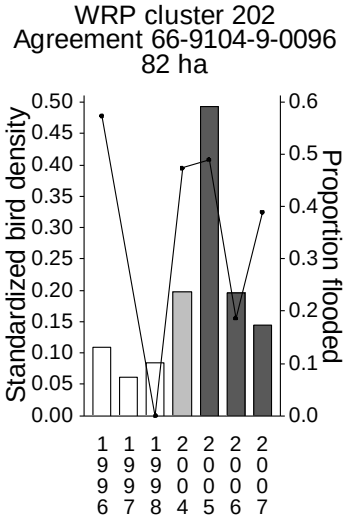

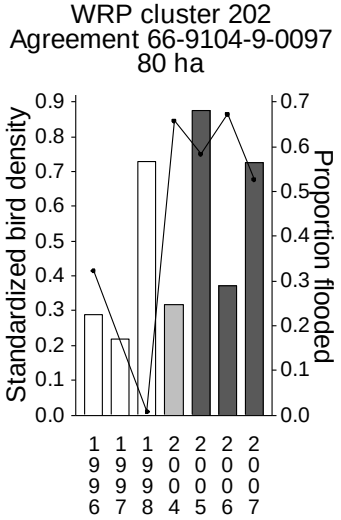

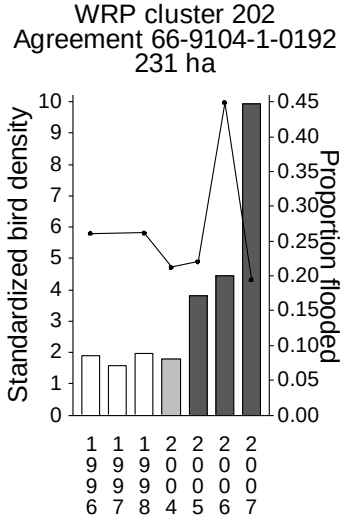

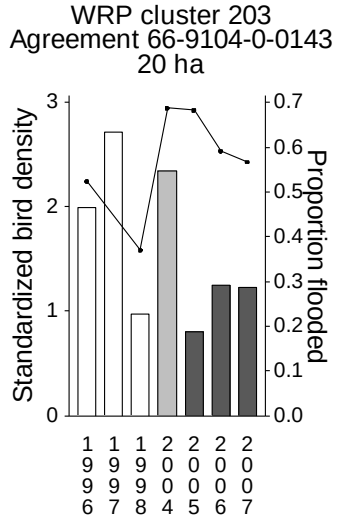

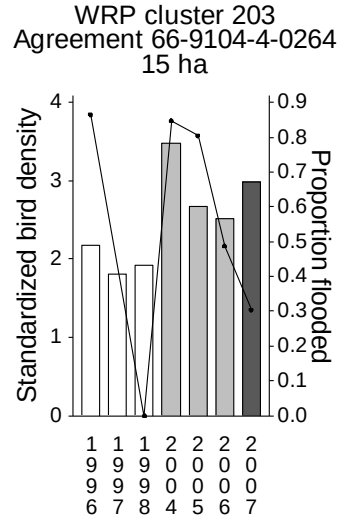

Appendix C. (continued). Annual variability in mean standardized bird density (bars) and the proportion of winter flooding (line) at WRP sites. Sites identified by cluster, agreement number, and size. Bar color denotes restoration status; white = pre-enrollment, light grey = enrolled, dark grey = post-restoration.

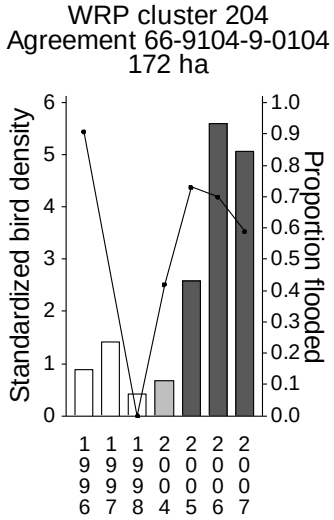

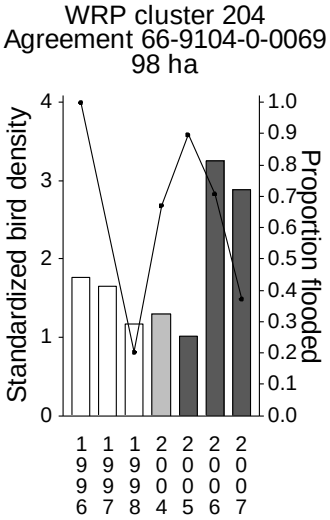

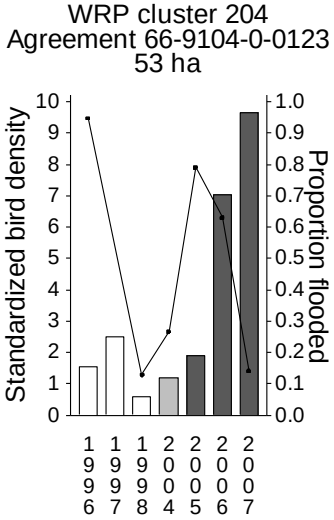

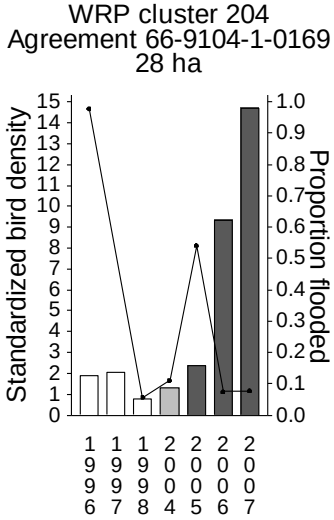

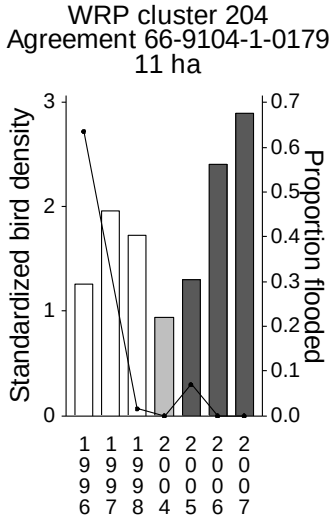

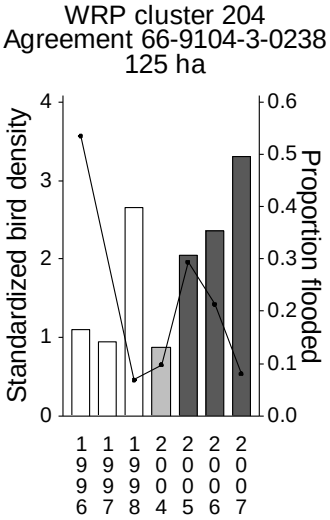

Appendix C. (continued). Annual variability in mean standardized bird density (bars) and the proportion of winter flooding (line) at WRP sites. Sites identified by cluster, agreement number, and size. Bar color denotes restoration status; white = pre-enrollment, light grey = enrolled, dark grey = post-restoration.

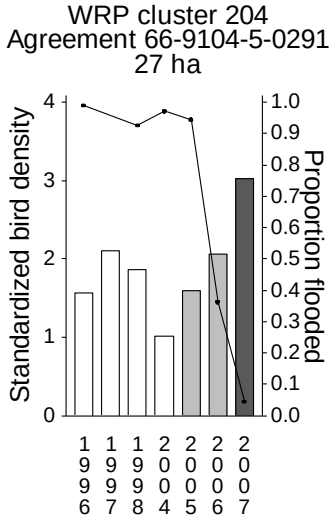

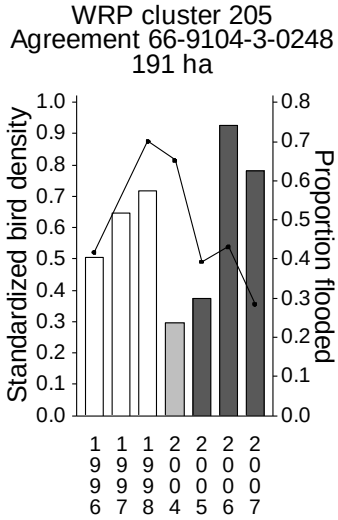

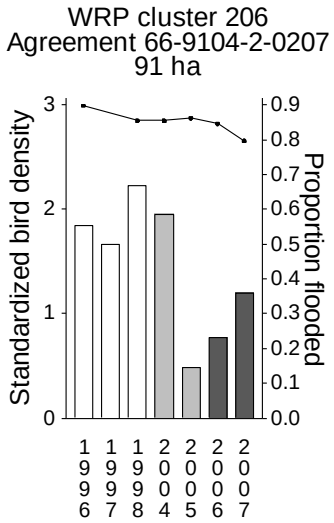

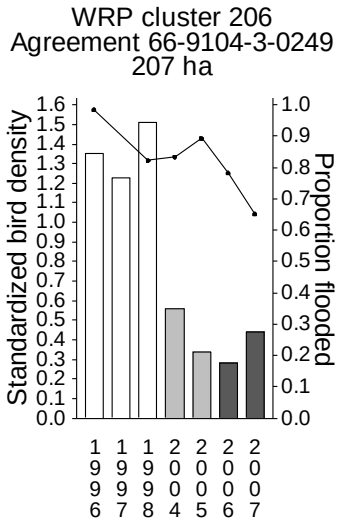

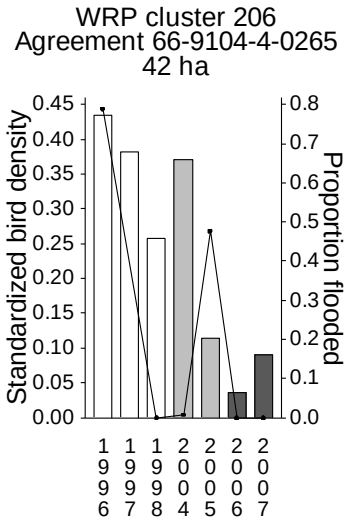

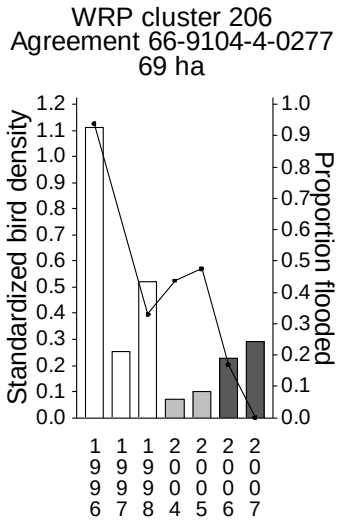

Appendix C. (continued). Annual variability in mean standardized bird density (bars) and the proportion of winter flooding (line) at WRP sites. Sites identified by cluster, agreement number, and size. Bar color denotes restoration status; white = pre-enrollment, light grey = enrolled, dark grey = post-restoration.

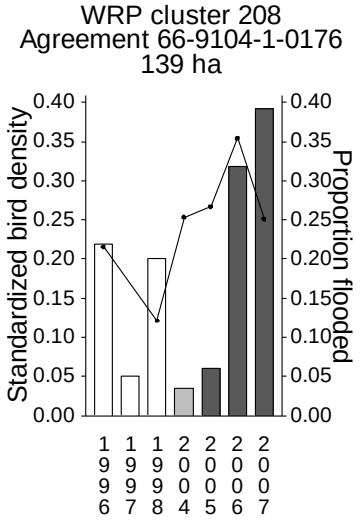

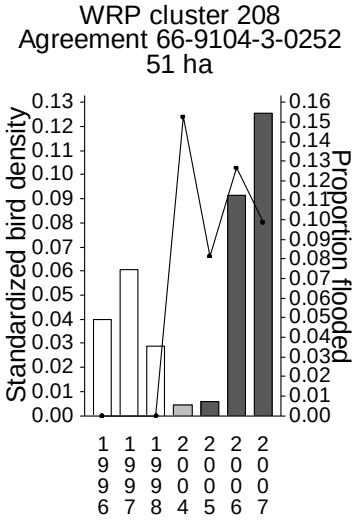

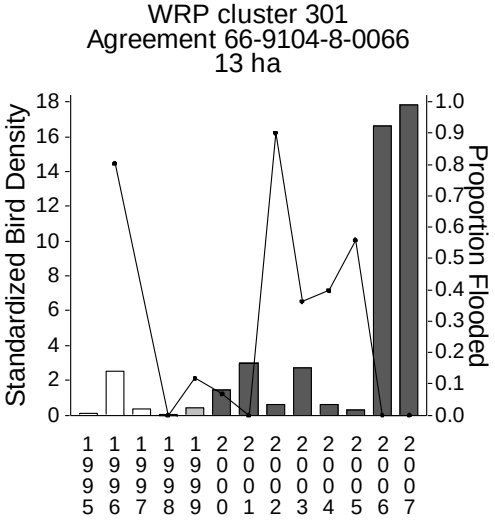

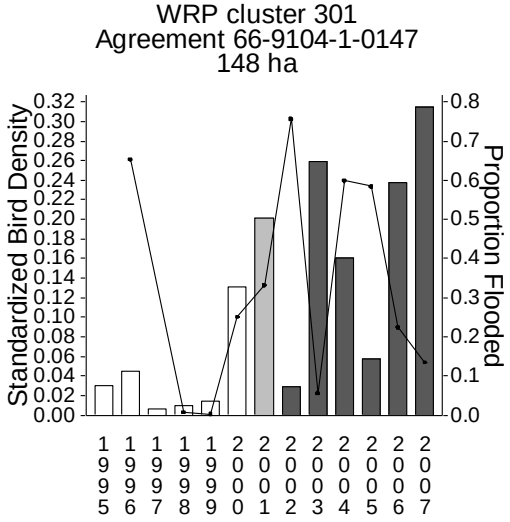

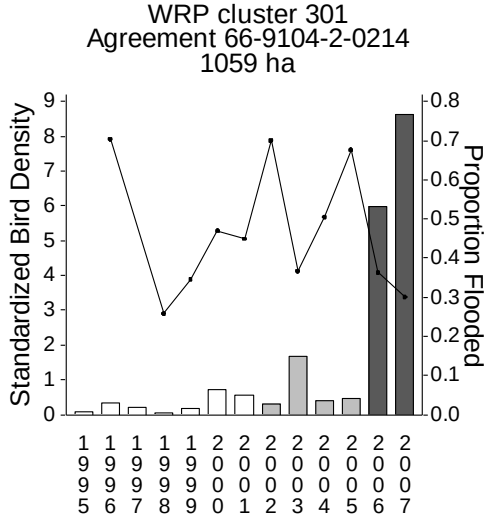

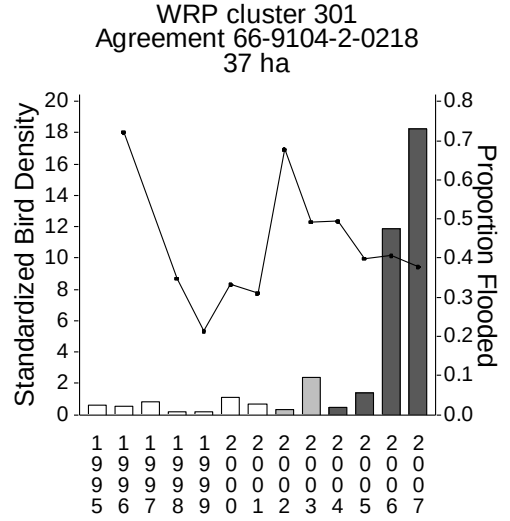

Appendix C. (continued). Annual variability in mean standardized bird density (bars) and the proportion of winter flooding (line) at WRP sites. Sites identified by cluster, agreement number, and size. Bar color denotes restoration status; white = pre-enrollment, light grey = enrolled, dark grey = post-restoration.

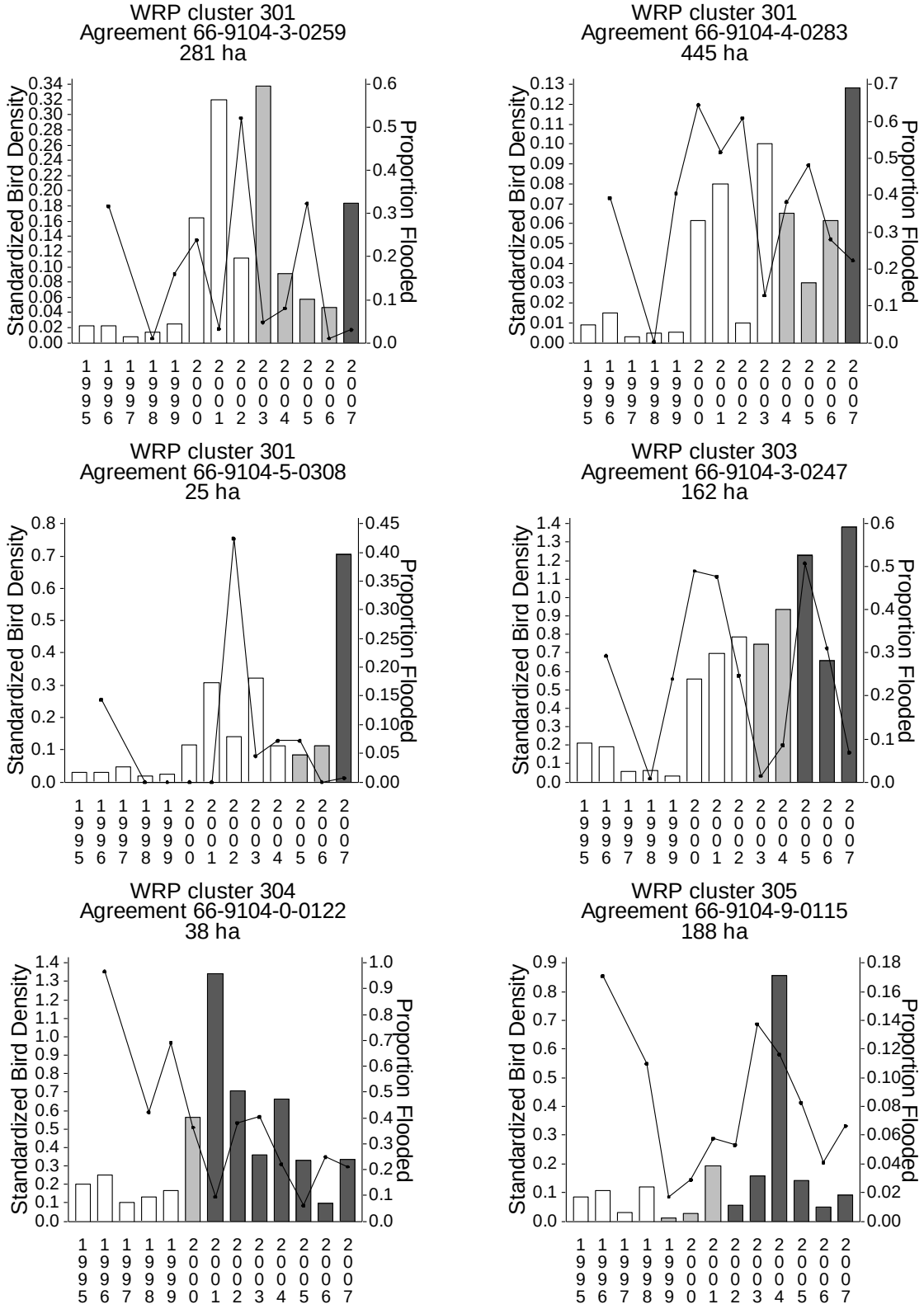

Appendix C. (continued). Annual variability in mean standardized bird density (bars) and the proportion of winter flooding (line) at WRP sites. Sites identified by cluster, agreement number, and size. Bar color denotes restoration status; white = pre-enrollment, light grey = enrolled, dark grey = post-restoration.

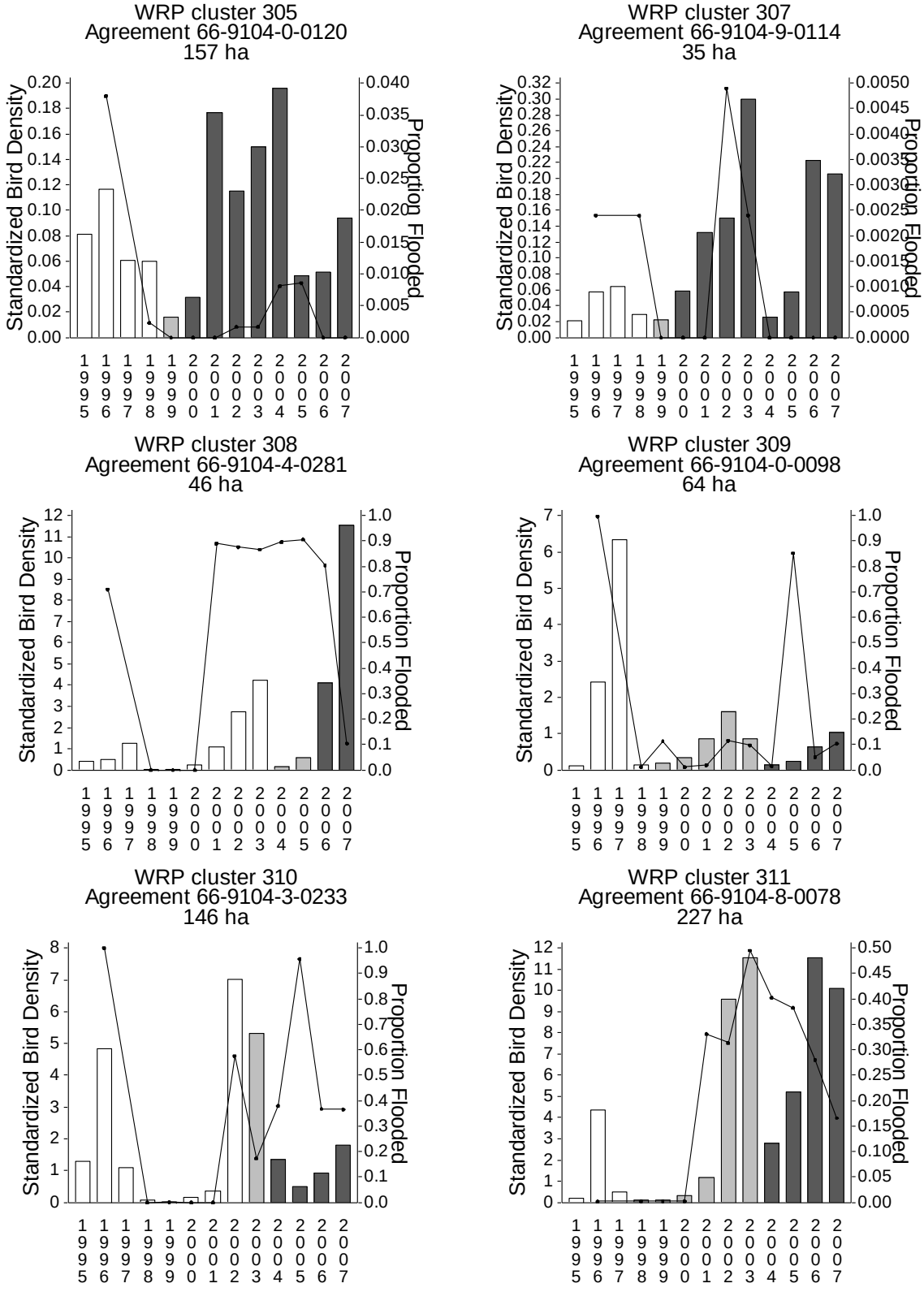

Appendix C. (continued). Annual variability in mean standardized bird density (bars) and the proportion of winter flooding (line) at WRP sites. Sites identified by cluster, agreement number, and size. Bar color denotes restoration status; white = pre-enrollment, light grey = enrolled, dark grey = post-restoration.

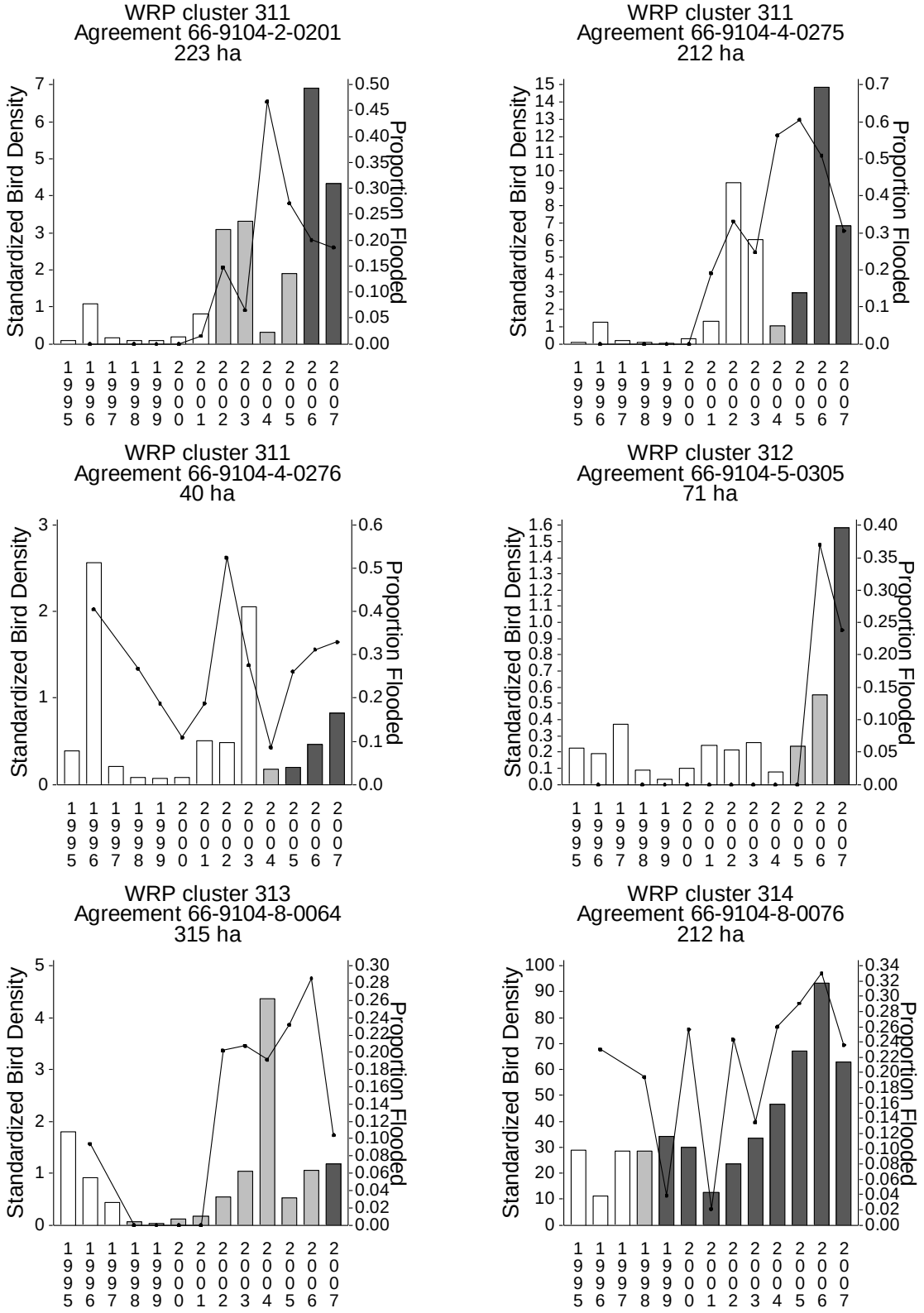

Appendix C. (continued). Annual variability in mean standardized bird density (bars) and the proportion of winter flooding (line) at WRP sites. Sites identified by cluster, agreement number, and size. Bar color denotes restoration status; white = pre-enrollment, light grey = enrolled, dark grey = post-restoration.